3-16-2012

The effects of temperature forcing on dengue dynamics via the extrinsic incubation period

Paula Danielle Weber

Paula Weber

Candidate

Mathematics

Department

This thesis is approved, and it is acceptable in quality and form for publication:

Approved by the Thesis Committee:

Helen Wearing , Chairperson

Pedro Embid

Monika Nitsche

The Effects of Temperature Forcing on Dengue Dynamics via the Extrinsic Incubation Period

by

Paula Danielle Weber

B.S., Mathematics, University of New Mexico, 2008

THESIS

Submitted in Partial Fulfillment of the
Requirements for the Degree of

Master of Science
Mathematics

The University of New Mexico

Albuquerque, New Mexico

December, 2011

Dedication

To my husband who supports, loves, and challenges me.
As well as to my parents who instilled in me at an early age a love for learning and were ceaselessly encouraging during my education.

Acknowledgments

I would like to thank my advisor, Professor Helen Wearing, for her tireless guidance and incredible insight during this process. Thanks to John Shadid, for the opportunity to work with and learn from him. I would also like to thank Harry Gullett and Reed Weber for their thoughts on the numerous revisions. Thanks to Jesus Christ who holds all things together.

The Effects of Temperature Forcing on Dengue Dynamics via the Extrinsic Incubation Period

by

Paula Danielle Weber

B.S., Mathematics, University of New Mexico, 2008

M.S., Mathematics, University of New Mexico, 2011

Abstract

Dengue fever is a mosquito-transmitted disease that is endemic in many parts of the tropical world and affects a significant proportion of the human population. Temperature is known to influence aspects of the dengue transmission cycle, which has consequences for disease dynamics. Previous work has explored the effects of temperature on the mortality rate of the mosquito and the resulting population change. However, there is substantial evidence that the extrinsic incubation period (EIP) of the pathogen within the vector host, *Aedes aegypti*, is also temperature dependent. This dependence has not been thoroughly researched. We present a single serotype compartmental model with a gamma-distributed exposed vector class to account for a temperature-dependent EIP. Where appropriate, temperature-dependent vector mortality is convolved with the temperature dependent EIP using the mortality function presented by Yang *et al.* [49]. Both seasonally and diurnal temperature changes are examined for their potential effects upon dengue persistence. The mean and range of temperature fluctuations that facilitate persistence are presented based

upon the EIP function, initial conditions, seasonal temperature forcing with and without vector mortality, as well as seasonal and diurnal temperature forcing with and without vector mortality. With seasonal forcing and temperature dependence only in the EIP, all simulations with mean temperatures above 26°C show persistence. However, if vector mortality is also variable, persistence is no longer possible in higher temperatures with higher temperature ranges. Diurnal forcing exacerbates this effect limiting persistence to mean temperatures of 23°C to 34°C with variable temperature ranges. It is clear that more data are needed to reduce the uncertainty in estimating the relationships between both EIP and vector mortality because these relationships can have large effects on disease dynamics. Additionally, this work demonstrates that when modeling temperature-dependent effects, it is vital to not only include seasonal variation in temperature but also diurnal variation.

Contents

List of Figures

List of Tables

Glossary

DDE	delay differential equation
DHF	dengue hemorrhagic fever
DSS	dengue shock syndrome
DTR	daily temperature range
EIP	extrinsic incubation period
ODE	ordinary differential equation
R_0	reproduction number

Chapter 1

Introduction

1.1 Dengue Epidemiology

Dengue fever is a disease that is the subject of much research in epidemiology. While a great deal is known about the pathogen that causes dengue as well as the vector that carries it, *Aedes aegypti*, there remain vast areas of research unexplored. Temperature is thought to be a major contributor to the dynamics of dengue infection. Most of the modeling of temperature dependence is relegated simply to the population size of the vector. However, it is known that the time which it takes the pathogen to render the mosquito infectious is considerably variable. Some measures have been made to quantify this variability, but this measure has not been studied to identify whether it is a major factor in dengue dynamics. This being the case we present a short review of what is known about dengue fever, examine the biology of the vector itself and its potential for temperature dependence, and review the available data on the length of time before the vector is infectious. We shall also present a short review of past studies on the climatological influence of dengue as well as temperature-dependence studies using different pathogens, and review previous dengue modeling as well as

the efforts to incorporate temperature. From this foundation we shall then develop our model which incorporates temperature-dependence in the vector biology as well as the variable EIP.

Dengue currently has the potential to affect two fifths of the world's population and is endemic in over 100 countries [32]. It is possible that due to increased temperatures, as a consequence of climate change, this proportion could increase because the primary vector of the disease is the mosquito, *Aedes aegypti*, whose geographic range may expand with an increase in temperature [17]. This increase in temperature may also contribute to a worsening in the severity of disease in certain regions. Factors that are thought to contribute to the severity of the disease are diverse and not well understood but may include: host genetics, nutrition, age, sex, and previous illnesses [13]. Symptoms of dengue resemble the flu and include mild to severe fever, headache and pain behind the eyes, muscle and joint pain, and rash. Thus the social impact of dengue fever is one of morbidity not mortality. Dengue hemorrhagic fever (DHF) and dengue shock syndrome (DSS) are, however, another matter. DHF has more severe symptoms of fever, abdominal pain, vomiting, and bleeding and is potentially fatal with a mortality rate as high as 20% and mainly affects children [16, 32]. Treatment is limited and there is no vaccine, but maintaining hydration is vital and medical intervention increases survival. Without a vaccine, controlling the disease and its spread is accomplished mainly through control of the vector *A. aegypti's* population size.

The history of the *A. aegypti* mosquito and the subsequent spread of dengue is an interesting one. *A. aegypti* was also the primary vector for yellow fever, and in 1915 the Rockefeller Foundation spearheaded an effort to eradicate Yellow Fever in the Western Hemisphere through the use of pesticides to wipe out the mosquito population [44]. Their efforts were very costly, but in the 1950's and 1960's they had achieved near eradication of the mosquito *A. aegypti* in urban South and Central

America. At this time the control measures were lifted, *Aedes aegypti* repopulated urban areas and is found worldwide in tropical and sub-tropical regions. With this growth in population we have seen an astonishing increase in both the frequency of epidemics as well as the severity. Although dengue was endemic, in that there was continuous and high incidence, in the Americas there were still only rare cases of DHF until the early 1980's. By the end of the decade, however, there were regular occurrences of DHF in every endemic country [16]. This is echoed by the World Health Organization: 40 years ago nine countries experienced DHF and now that number has quadrupled [32].

Dengue is caused by a virus that is subdivided into four serotypes: DEN1, DEN2, DEN3, DEN4. The human body recognizes each serotype as a distinct virus, so while the symptoms are the same and each is considered dengue, a person could be infected with four strains of dengue sequentially. A person after being infected with DEN1 acquires lifetime immunity to DEN1, but is susceptible to DEN2, DEN3, and DEN4. There is thought to be some measure of cross-immunity that may decrease over a matter of months after exposure which means that for several months after being infected with DEN1, an individual is unlikely to be infected with the other serotypes, but this protection wanes. It is also interesting to note that DSS and DHF are observed where two or more serotypes are epidemic, or serially epidemic [18]. In epidemiology, a very important measure of a pathogen's fitness is the reproduction number, R_0, which is the average number of secondary infections due to one infection in a completely susceptible population. An R_0 less than one will not result in an epidemic and the pathogen will not persist. Estimates of the reproduction number for dengue range from 0.49 to 11.6 [18]. However, for areas of high endemicity it is thought to lie in the range of 4.3-5.8 [6].

1.2 The Mosquito: *Aedes aegypti*

The primary vector of the Dengue virus is the mosquito *Aedes aegypti*. Like all other mosquitoes, it goes through four life stages: egg, larva, pupa, and adult; only adult females take a blood meal. In this study we will not consider transovarial transmission to be a factor because, although it has infrequently been observed in the lab, it is extremely rare in nature. Khin examined this phenomenon finding two cases out of 16,258 mosquitoes, but both were male [23] and as they were male they could not transmit dengue because males do not take blood meals.

1.2.1 Bloodmeals and Biting

Dengue is spread from the human host to the mosquito during the blood meal. Once the mosquito has become infectious, each subsequent human host upon which it feeds will be infected with dengue. The first blood meal is often taken 23 or 24 hours after emergence, but has been observed as early as 21 hours after emergence from the pupa life stage into the adult stage [21]. Females are capable of multiple bloodmeals in their lifetime, some as early as 2-5 hours after the first blood meal [21], and as the mosquito ages it is no less capable or likely to take a blood meal [35]. The frequency of taking a bloodmeal is connected to the mosquito's oviposition frequency; in order to lay eggs the female must first imbibe a bloodmeal and mate. However, it has been hypothesized that at temperature extremes the meal may be used for the mosquito's survival instead of oviposition [9]. Males primarily feed upon fruit which is also a food source for females, but in the lab females are primarily fed using sugar cubes or a sucrose solution [27, 30, 35]. In a study that captured female mosquitoes that were attempting to bite, recaptures of the same mosquito indicate a four day gonotrophic cycle with secondary (as well as tertiary) feeding occurring every two days [8]. There have been numerous studies on the biting rate of *A. aegypti*

in multiple locations, some with conflicting results. An increase in temperature in Thailand resulted in a significant increase in blood feeding, but this was not found in Puerto Rico [39]. It appears that the biting rate may be geographically dependent and may be influenced by multiple factors including temperature. Biting peaks often occur either mid-morning or mid-afternoon but biting can occur at any time of day as opportunity allows [2, 31, 43]. However, there appears to be consistency in that the majority of biting activity occurs in the temperature range of 25-35°C with an optimum close to 35°C [29, 31]. Identifying the peaks of biting can be important as it can be used to help target and reduce the risk of bites during these periods [31]. Other activity of the mosquito is also temperature dependent. *Aedes aegypti*'s range of activity is also temperature dependent, normal flight is not seen below 21.1°C. Flight is possible but limited and clumsy below this range until 10°C where very little activity is observed and no flight occurs [38]. Reduction in flight and activity has the potential to effect the survival of the mosquito as well as the transmission of dengue.

1.2.2 Oviposition

An increase or reduction in oviposition will affect the mosquito population size in the future. *A. aegypti*'s eggs are laid in standing water, often in objects such as tires or cans or in pools of water [45]. The eggs can survive large variations in temperature (as well as availability of water) making them a hearty species. Eggs can survive sustained temperatures of as low as 8.9°C and as high as 43.3°C [42, 41]. However the majority were killed when maintained for seven days at or below a temperature of 15.6°C [42]. It was found by Costa *et al.* [9], that at high temperatures (35°C) fewer eggs were laid per mosquito but again this was slightly counteracted by humidity. In general, humidity allowed for more eggs to be laid than low humidity and increased temperature decreased the amount laid to various extents.

Table 1.1: Mean number of eggs laid per mosquito

Temp(in°C)	low humidity	high humidity
25	85.99	99.08
30	82.89	75.75
35	54.53	59.62

1.2.3 Development

At each stage of development the mosquito is under predatory and caloric pressures. In one study the number of mosquitoes that survived from egg to adult was correlated directly with the amount of food and only to a small degree with the availability of water [19]. It was found that activation began after two weeks with an average temperature of 18.3°C [42]. Average weekly temperatures below 15.6°C killed most larvae but some survived in temperatures as low as 8.8°C [42]. If eggs are not activated, even if they are without water for an extended period of time, it is possible for these eggs to fully develop once temperatures are again high [19, 42].

1.2.4 Adult Mortality

The mortality of the mosquito is very important, both in the total population size and in the ability of the pathogen to render the mosquito infectious (see section 1.3). *A. aegypti* reared under lab conditions can live an extraordinarily long time, some as long as 225 days [38]. In nature, however, females survive 15 days on average with a maximum of 42 days (Korovitskii and Artemenko according to Schoof [38]). Different population models choose differing averages, some with a conservative 15-20 days [7] and others as low as 8.6 days [18]. Some stochastic models choose to take the maximum day of survival to be 45 days with a survival rate in the range of (.8-.95) [3] or a lower survival rate of (.87-.91) with no maximum lifespan. Some field studies give a survival rate of as low as .656 [8], but this may be low due to the

nature of the data: it was limited to females who are feeding again during a short time span. Elevated temperature also has an effect on mortality for adults. 100% of adults were killed after 30 minutes of exposure to 46.1°C as well as 15 minutes of exposure to 48.9°C. All stages of Aedes aegypti can survive extended periods in temperatures of 40.6°C [41]. In another study, Rohani and colleagues found mortality rates for dengue-infected mosquitoes (values for DEN2 and DEN4 are given) for temperatures 26, 28, 30°C to be 20-25%, 30%, and 40-45% respectively. Increased temperature decreased the mosquito's lifespan and reduced oviposition, but there was also a link between high and low humidity where high humidity would offset to various degrees the negative effects of high temperature [9]. Different strains of *A. aegypti* have different mortality rates as well when maintained at the same constant temperature [27]. Mortality/survivorship rates contribute to the dynamics of the adult population size, but they are by no means the only factor because of the life stages of the mosquito.

1.2.5 Other Environmental Effects

It is thought that "the amount of rainfall may or may not affect the population size depending upon the normal state of the location in question. If it is typically dry then an increase in rain often produces an increase in the vector population. However, if a locale is generally very wet then the seasonal upswing in rain may not increase the population dramatically but may instead affect the adult survivorship and feeding activity" [18]. Again seasonal fluctuations of a population may be geographically dependent as well, in that cold may reduce the typical range of the mosquito (in both altitude and laterally/longitudinally) as it is dependent on the normal state of the location and temperature and rainfall. Drought may not affect the range of *A. aegypti* but rather its density or vice versa [44].

1.3 Extrinsic Incubation Period (EIP)

The extrinsic incubation period (or EIP) of a virus is the length of time from the mosquito's acquisition of the disease until it is infectious and thus able to transmit the disease to another host. Different methods are used to determine EIP. The method that makes the most sense biologically starts with the mosquitoes being offered a bloodmeal by an infectious host. Later these mosquitoes are allowed to feed on a different host and this host is examined for transmission of the disease. It is also customary to sacrifice a small number of the exposed mosquitoes periodically to examine if there is virus present in either its abdomen, salivary glands, or both. The virus can not be transmitted until it reaches the salivary glands, a necessary but not sufficient qualification. The work by Watts *et al.* uses the method of testing an exposed host. They used both a high and a low dose in the initial feeding of the mosquitoes [45] for DEN2. McLean *et al.* used a similar procedure, also using DEN2, but in one of the trials they directly injected infected blood into the mosquito's abdomen, which has been noted to inaccurately accelerate the EIP [30]. This acceleration is due to the process itself, by injecting directly into the mosquito's abdomen the entire process of the virus passing from the mouth piece to the gut is overlooked. In this way it is not reliable to determine the EIP and is not an appropriate proxy for it either given that other data are available. In the trial using the feeding procedure, at the lowest temperature (12.9°C), the mosquitoes would not bite but the pathogen had reached the salivary glands. Rohani *et al.* periodically sacrificed exposed mosquitoes and determined if virus had reached the salivary glands or not. They conducted experiments with both DEN2 and DEN4 [37].

Table 1.2: EIP as a function of temperature in days with the methods described in section 1.3. *** denotes presence of virus in mosquito but feeding did not occur at that temperature. > denotes no host was infected during the duration of the study and the length of the study is given.

Temp.°C	Watts-high	Watts-low	McLean-feeding	McLean-Injection	Rohani-DEN2	Rohani-DEN4
12.9			35***	13		
20		>25				
23.9				23.9		
24		>25				
26	>25	>25			9	9
26.7			13	10		
28					9	9
30	12	25			5	5
32	7					
32.2			6	6		
35	7			3		

1.4 Climatological Factors and Dengue Incidence

Considering the biology of the disease and the mosquito, there is a profound potential for variation and complexity. The biology of the vector leads many experts to conclude that rainfall and temperature contribute the greatest influence to the dynamics of dengue by the effect on the mosquito population, its life cycle, mortality rate, and the disease's EIP [18]. Temperature alone could have a major impact on oviposition, hatching, pupation, emergence, mortality, and transmission [5]. As described in sections 1.2 and 1.3, studies have attempted to quantify some of these potential influences.

Other studies take a reverse engineering perspective and instead look at past records of dengue incidence in a region and (most often) the weather patterns associated with the time and location. One such study looked at El Niño (or El Niño Southern Oscillation or ENSO) effects in Thailand, Puerto Rico, and Mexico over a period of 13-20 years (depending on location) using Wavelet analysis [20]. El Niño and epidemics in the regions cohered on the annual scale but not on the multi-year scale demonstrating a seasonal forcing of dengue but not a direct forcing due to El

Niño. Another study looked at multiple aspects of weather (land/sea temperature, rainfall, humidity) and their contribution to vector populations (BI or breteau index which is a method of estimating a location's mosquito population size) and dengue incidence in Taiwan [25]. It was found that dengue fever admissions and high BI did not coincide at the same period of each year but in years with large epidemics there was an above average BI. A study by Chowell and Sanchez looked at the 2002 Colima, Mexico epidemic and five climatological factors [7]. The factors examined were precipitation, evaporation, maximum, minimum, and mean temperature; each was considered with variable time lags of one to three months. They found that each factor had the highest correlation with dengue incidence with different lags, but that the greatest correlation existed between minimum and mean temperature and precipitation. A similar study looked at reported cases in Taiwan for the years 2001-2008 [5]. They considered rainfall, maximum, minimum and mean temperatures and found that rainfall and minimum temperature with a lag of three months and one month respectively were significant. In this study it was also noted that minimum temperature had the greatest effect and was most significant. Another study looked at biting rates and the possible effects temperature may play over a year [50]. Data were collected in the same location weekly over the course of a year; the maximum temperature did not change much although the minimum did. It was found that the correlation coefficient between biting rate and the minimum temperature was significant and may have accounted for the seasonality of biting. Researchers now conclude that lowest daily temperature, instead of average daily temperature may be the strongest influence in dengue transmission [18].

1.5 Temperature Dependence of Other Diseases

Many diseases are temperature dependent due to the biology of the vector or the pathogen itself. Malaria has a more complicated life cycle than dengue in that it requires sexual reproduction inside the vector before rupturing the mosquito stomach and moving to the salivary gland to infect any subsequent humans fed upon. Malaria has a temperature dependent EIP in which changes as small as 2°C have a significant impact. It was found that a constant temperature of 18°C led to an incubation period of 46 days but with diurnal fluctuations of ± 7°C it was reduced to 32 days. Too much of an increase in temperature had the opposite effect; mean temperatures above 24°C increased the incubation period [34]. These results imply crucial changes in the strength and geographic bounds of malaria due to climate change.

A study by Reisen *et al.* examined West Nile virus and specifically the NY99 strain. They found the zero transmission temperature (14.3°C) and found a marked shortening of the EIP with increasing temperature. Also, small differences in the temperature had significant consequences for the likelihood of transmission, leading to the conclusion that certain locations had a much higher likelihood of an epidemic than others. For example, with normal temperatures, Long Beach and Monrovia in California have EIP's of 17.9 and 12.4 days respectively, but the shortened EIP doubles the infective lifetime of the mosquito in Monrovia [36]. Another study looked at two strains of West Nile disease and found that the WN02 strain was much more virulent in higher temperatures than NY99. When considering the degree days and incubation rates, while the typical degree day is defined as $DD = tT$ (where DD is degree day and t is time in days and T is temperature in °C) a quartic function ($DD = tT^4$) is much more representative of the data and thus a small change in temperature results in a highly significant change in infection capability [24].

Temperature dependence is a general phenomenon that plays a significant role in

the dynamics and resulting epidemics of many diseases.

1.6 Previous Modeling of Temperature Dependence in Vectored Disease Systems

Strictly considering the population of *A. aegypti*, Dye determined an appropriate continuous-time population model of the vector and found that adult survivorship is the most sensitive parameter, more so than birth rate or availability of breeding sites [10]. An SEIR, SEI (susceptible, exposed, infectious, recovered - see Fig. 2.1 and Fig. 2.2) compartment model is used with two serotypes in another model [33]. It is a stochastic model with some temperature dependence, but this is in play only in the population dynamics of the vector through its life stages. The timing of introduction of an infectious human was variable and it played a major role in the size of the resulting epidemic. During the winter months no epidemic ensues but the further into the summer the infection is introduced the larger the resulting epidemic. Another study, also using a two serotype compartmental model, included seasonal forcing on biting, EIP estimates, and larval mortality rates in conjunction with seasonal data from Bangkok [4]. Biting rate and mortality was found to have a significant effect.

A different study looked at the vector capacity with temperature dependent survival rate and EIP [3]. The gonotrophic cycle was temperature dependent as well as the mortality rate. The EIP was not temperature dependent, but it was varied within a range of 4-24 days to determine when the first and subsequent infectious bites would be possible, if ever, due to the mortality rate in the mosquito.

Another set of studies focused on the temperature effects on the vector population as well as its oviposition rate or the frequency of biting [47, 48, 49]. These studies

looked at temperature dependent mortality rates and hatching rates for each stage of the vector and then the resulting effect on the rate at which female mosquitoes oviposit.

A similar study using a different vector (*Aedes albopictus*) used a temperature-dependent stochastic population model of the vector with a constant temperature EIP [11, 12]. The ability of a mosquito to transmit the disease is determined by the time at which the mosquito takes an infected blood meal. It then tracks the amount of time determined by the EIP based on the temperature and then the model determined the time required before its next blood meal, this is its first infectious bite. Subsequent bites are possible depending on the mortality rate and time at which the mosquito took its first infectious blood meal in its life cycle. This model was able to accurately detect the early season spikes as well as the end of season die off of the mosquito populations based on the climate and temperatures for the region studied.

In a series of studies, Focks *et al.* developed a simulation model of a mosquito population (CIMSiM) using a large number of input parameters including type and number of water containers, max/min temperature, relative humidity, availability of food, and so on to be used in conjunction with a compartmental model of disease [13, 14, 15]. The population model has used numerous locations and climates with reasonable success. The adult mosquito population size, as well as the size of the mosquitoes themselves, are parameters passed to the DENSiM simulation as mosquito size is thought to influence biting rate. DENSiM uses the four serotypes and assumes infection from one serotype gives lifelong immunity to that serotype and temporary (several months) immunity to the other serotypes, a temperature dependent EIP is used. Daily survivorship and EIP thus interact nonlinearly and are the driving force in the disease dynamics. It was found that the onset was not affected by the adult population size so much as a reduction in EIP, however titer

strength (or the amount of virus in the infected blood meal) also contributes.

A model has also been developed that is driven by climate to predict dengue using a region's local forecasts of weather (temperature and precipitation primarily) to predict regions in a country that may experience epidemics up to five months in advance. Under and over predicting of incidence was observed, but this can only be improved with more data both quantitatively and qualitatively [28].

As one can see, a great deal of work has begun to investigate temperature dependence in dengue incidence. However, these models use a variable population size allowing temperature to drive the population size of the mosquito. In most cases this is the only means in which temperature acts upon the system. A handful of models used a variable EIP but not as a function of temperature. Only one model used a temperature-dependent EIP (Focks *et al.*) which is a constant value except at temperature extremes in which it is cut-off. We shall develop a model that considers temperature-dependent EIP as well as temperature dependent vector mortality. With this framework we will explore the impact of the variable EIP and attempt to determine if this is a significant factor in dengue transmission and if it allows persistence of the disease where mean temperatures might otherwise suggest it would not.

Chapter 2

Methods

We will build a model based upon the typical indirect transmission compartment model used in epidemiology. We will modify it to accommodate a variable incubation period in the vector. The incubation period will be temperature dependent based upon the data presented in section 1.3. In addition, the mortality of the vector optionally can be temperature dependent and this function will be presented. All parameters used in the model are summarized in table 2.1 at the end of section 2.2.

2.1 Model Framework

Compartment models divide the host and vector populations into multiple categories or classes. The simplest model is the SI compartment model which represents the members of the population that are susceptible (S) and infectious (I). The number of compartments is dependent upon the biology of the organism involved. The human host is represented by the SEIR model (see Fig. 2.1) which is broken into four classes of susceptible (S), exposed or latent (E), infectious (I), and recovered (R). The vector, on the other hand, is infectious until its death and is therefore represented by the

SEI model (see Fig. 2.2) [1]. Only the female vector population is modeled as only females take bloodmeals and are thus capable of transmitting dengue.

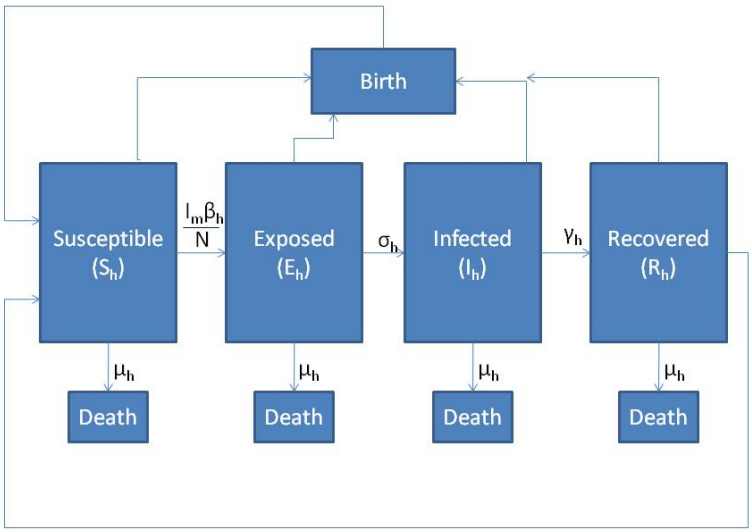

Figure 2.1: SEIR flow diagram representative of human population

Members of the host as well as the vector populations move from compartment to compartment based on different rates and the dynamics can therefore be represented as a system of ordinary differential equations (ODE's) (eqn. 2.3 and 2.4). Our model assumes a constant population size and so the death rate (μ) is equal to the birth rate. Members of the susceptible population move to the exposed class at the (transmission) rate ($\frac{\beta I}{N}$). The system of equations for each organism is coupled by transmission as the mosquito infects the human and the human infects the mosquito. The exposed population then moves to the infected class after passing through the latent period at a rate (σ). This latent period in the vector population is the EIP and is therefore not constant but temperature-dependent. If the recovered class exists then the members of the infectious class move into it at the recovery rate (γ).

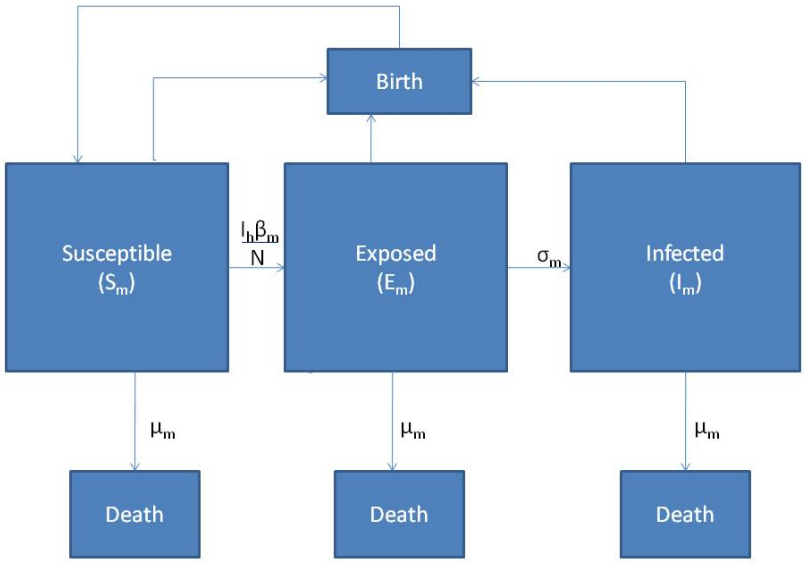

Figure 2.2: SEI flow diagram representative of mosquito population

2.2 Model Parameterization

2.2.1 Temperature Dependent EIP Function

For development of the EIP function we took the various data sets as described in section 1.3 and used nonlinear least squares to fit the function $A \exp BT$ where A and B are unknowns and T is temperature. Each data set yielded a different function, each of which may be specified in the model. We then used all of the data sets (excluding the McLean injection data), and for the data points in the lower temperature regions that require longer than 25 days to reach infection a length of 45 days was used. The fit and all the data points are included in Fig. 2.3. Some model development was pursued with each of the data fits, but unless otherwise noted $\tau = 25597.18 \exp(-.26197T)$ is the EIP temperature-dependent function used.

To examine a temperature-dependent EIP, one must modify the transition from the exposed class to the infected class. Instead of the newly infected mosquitoes moving from the susceptible class to an exposed class and finally to an infective class, one could instead introduce a time delay and thus use a delay-differential equation. The infective population would then be a function of (t-τ). There are standard techniques for solving dde's when τ is constant. However, τ is temperature-dependent, and thus a time-dependent function. This approach is flawed because it requires additional measures to bookkeep or maintain records of vector status. An example can be seen in a vector population moving in to the exposed class with an EIP of 14 days. After five days the temperature increases such that the EIP is now seven days. The population that entered five days ago has progressed in the cycle and would now see an acceleration in EIP as well, but how is this to be handled? Is it appropriate to now consider these mosquitoes to have an EIP of five days and to have progressed as far as $\frac{5*5}{14}$ days into the five day EIP period? What if the EIP shortened to two days? Would these mosquitoes all be infective? A different

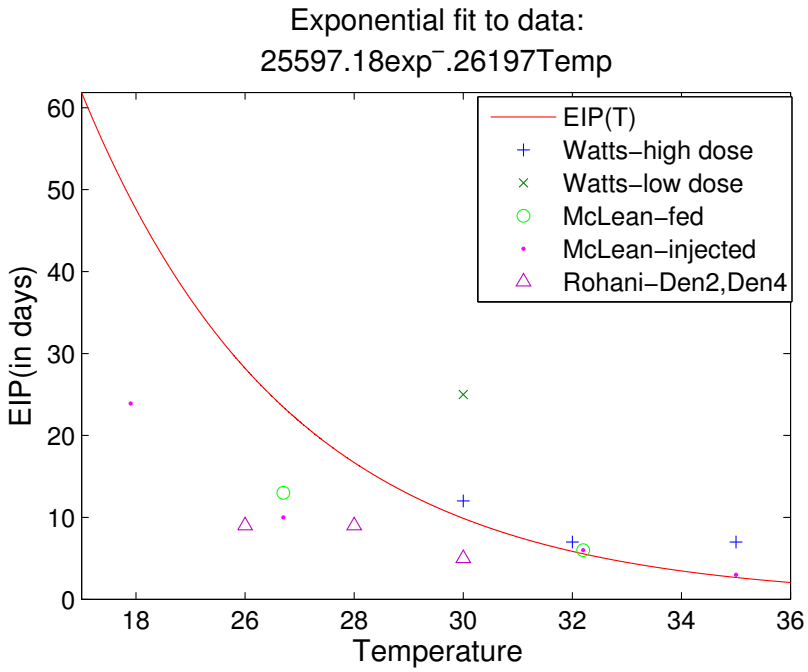

Figure 2.3: Data points from multiple EIP data sets with exponential function fit: $\tau = 25597.18 \exp^{(-.26197T)}$. This is the EIP function used for the various models unless otherwise indicated.

construction is needed for the exposed mosquitoes which takes this variation directly into account.

Instead we introduced a gamma distribution for the time spent in the exposed class which modifies Fig. 2.2 to Fig. 2.4. In the simple case, n=1, a gamma distribution is in fact an exponential. This would correspond to continuous movement from the exposed to the infective class with no time delay. At the other extreme, $n \to \infty$, the gamma distribution approaches a delta function which would correspond to an exact time delay of τ days, so the time spent in the exposed class would be described by a step function. To determine n we took the data of the number of mosquitoes that had infective salivary glands for each day sampled as given by Watts *et al.* [45] and fit a gamma distribution to determine n for each data set. The results were n=14.8

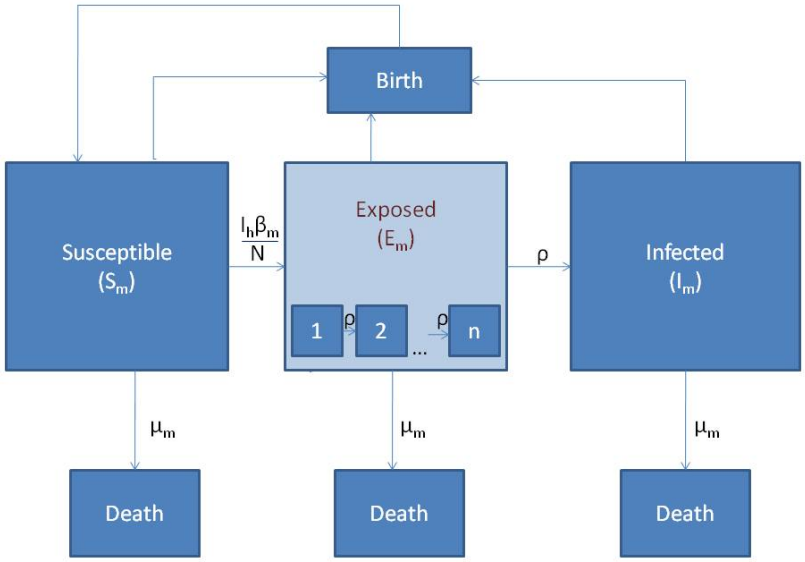

Figure 2.4: SEI flow diagram (without coupling) representative of mosquito population with gamma function used for exposed class

for 26°C, n=24.6 for 30°C, n=12.5 for 32°C, and n=8.4 for 35°C. For this study we chose to use n=10. There are therefore n sub-stages of the exposed mosquito class and the mosquitoes move through these stages at a rate of $\rho = \frac{n}{\tau}$ which could be useful in a stochastic model as other findings develop [46].

2.2.2 Temperature-Dependent Mosquito Mortality

The mosquito's lifespan is influenced by many factors, a reasonable but more stringent mortality rate of $\frac{1}{14}$ (1/day) was considered when vector mortality was not assumed to be temperature dependent. In the work by Yang *et al.* [49] they found the function $.000003809T^4 - .0003408T^3 + .01116T^2 - .159T + .8692$ to represent their data the best. This same function was used in our calculations when vector mortality was assumed to be a function of temperature (see Fig. 2.5). The inverse of the rate of

mortality is of course the average lifespan (see Fig. 2.6). Based upon other readings (see sect. 1.2), the length of survival in the temperature range of (17-32°C) may be higher than what is found in the field. These mortality rates do not consider predation and allow for ample feeding. Female mosquitoes, in particular, may experience a higher death rate while feeding. This function has extremely high mortality rates at temperature extremes, but mosquitoes have been noted to change activity levels in order to survive (such as seeking shelter and shade when it is very hot). Therefore with further data this function may be modified to have higher values in the nominal temperature ranges and reduced at the extremes. The average mortality rate for the temperatures we were looking at given this function is $\frac{1}{27}$ per day, so this mortality rate was also used when vector mortality was not to be temperature dependent, but it is noted when this is the case.

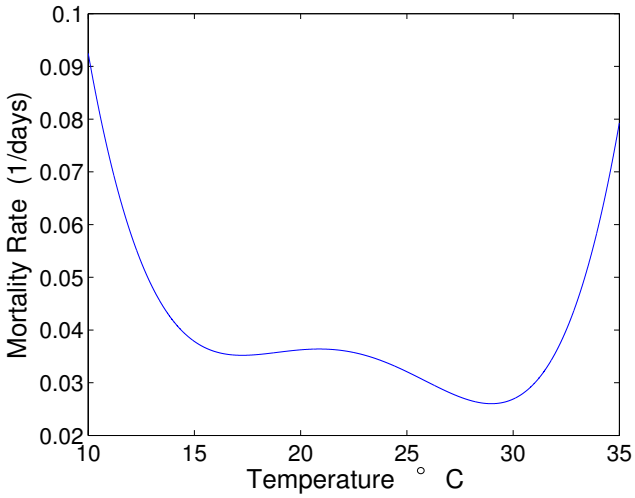

Figure 2.5: Vector mortality function used, as presented by Yang [49]

A conservative estimate of $\beta = \frac{70}{365}$ was used in this model, however, some authors use a β as large as .75 [4]. The average human lifespan was taken to be 60 years. The human intrinsic incubation period was taken to be five days which is well within the

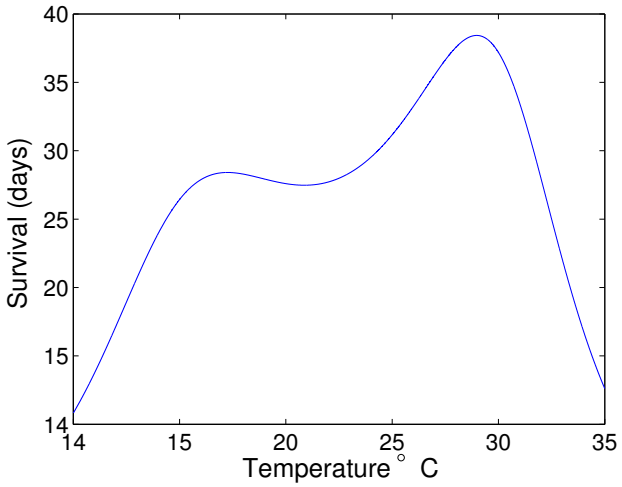

Figure 2.6: Vector survival based on Yang's mortality function

range of 4-10 days given by Siler [40]. Large population sizes were assumed because deterministic compartment models are inappropriate for considering the dynamics of small populations which are sensitive to stochasticity.

2.2.3 Temperature

The temperature forcing $T = T_1 + T_2$, on a yearly scale, where T_1 represents the seasonal forcing and T_2 the daily forcing was given by the function

$$T_1 = -A \cos \frac{\pi(t + t_1)}{180} + M \tag{2.1}$$

where A is the amplitude or half of the temperature range, M is the mean yearly temperature, t is time in days, and t_1 allows the user to start at varying time of the year by shifting the peak temperature: winter=0, spring=91, summer=182, fall=274. If a diurnal forcing was also being used then the function used for daily temperature variation was

$$T_2 = -DTR \sin 2\pi t \tag{2.2}$$

where DTR is the daily temperature range (9.44°C for all simulations). This range was used based upon the average DTR for three cities in Central and South America and then this was converted to °C. If diurnal forcing was used then temperature was the sum of eqn.2.1 and eqn.2.2.

Table 2.1: Model Parameters

Coefficients for equations	Value	Reference
n	10	Maximum likelihood using the salivary gland data of Watts [45]
$\tau(T)$ - linear	$\tau = \frac{-5}{4}T + \frac{183}{4} days$	Line through data of Watts *et al.* [45]for temps 26-32
$\tau(T)$ - exponential	$\tau = 97.177e^{-.0795*T}$	Nonlinear least squares using Mclean *et al.* feeding data [30];
$\tau(T)$ - exponential	$\tau = 126.9373e^{-.1006*T}$	Nonlinear least squares using Rohani *et al.* [37];
$\tau(T)$ - exponential	$\tau = 500.1015e^{-.1265*T}$	Nonlinear least squares using Watts *et al.* [45];
$\tau(T)$ - exponential	$\tau = 25597.18e^{-.26197*T}$	Nonlinear least squares using multiple data sets;
ρ	$\frac{n}{\tau}$ 1/days	
μ_h	$\frac{1}{60*365}$ 1/days	avg life expectancy
β_h	$\frac{70}{365}$ 1/days	transmission rate
σ_h	$\frac{1}{5}$ 1/days	avg duration of latent period[40]
γ_h	$\frac{1}{6}$ 1/days	recovery rate
N_h	500,000	human population size
N_m	1,000,000	mosquito population
β_m	$\frac{70}{365}$ 1/days	transmission rate
$\mu_m - high$	$\frac{1}{14}$ 1/days	avg life expectancy
$\mu_m(T)$	$.000003809T^4 - .0003408T^3 + .01116T^2 - .159T + .8692$	1/days life expectancy given by Yang *et al.* [49]
$\mu_m - low$	$\frac{1}{27}$ 1/days	avg life expectancy of Yang function for given mean temperatures

2.3 Equations

2.3.1 Coupled SEIR and SEI Systems

Human SEIR system

$$\begin{aligned}
\frac{dS_h}{dt} &= \mu_h N_h - \left(\frac{\beta_h I_m}{N_h} + \mu_h\right) S_h \\
\frac{dE_h}{dt} &= \frac{\beta_h S_h I_m}{N_h} - (\mu_h + \sigma_h) E_h \\
\frac{dI_h}{dt} &= \sigma_h E_h - (\mu_h + \gamma_h) I_h \\
\frac{dR_h}{dt} &= \gamma_h I_h - \mu_h R_h
\end{aligned} \tag{2.3}$$

Mosquito SEI system

$$\begin{aligned}
\frac{dS_m}{dt} &= \mu_m N_m - \frac{\beta_m I_h S_m}{N_h} - \mu_m S_m \\
\frac{dE_{m,1}}{dt} &= \frac{\beta_m I_h S_m}{N_h} - (\mu_m + \rho) E_{m,1} \\
\frac{dE_{m,2}}{dt} &= \rho E_{m,1} - (\mu_m + \rho) E_{m,2} \\
\frac{dE_{m,3}}{dt} &= \rho E_{m,2} - (\mu_m + \rho) E_{m,3} \\
&\vdots \\
\frac{dE_{m,n}}{dt} &= \rho E_{m,n-1} - (\mu_m + \rho) E_{m,n} \\
\frac{dI_m}{dt} &= \rho E_{m,n} - \mu_m I_m
\end{aligned} \tag{2.4}$$

2.3.2 Non-Dimensionalization

To normalize and simplify the equations used, we first chose to non-dimensionalize the coupled system. We non-dimensionalize by scaling the population variables by total population size and time by human lifespan.

Nondimensionalize using:

$$\begin{aligned} T &= \mu_h t \\ S_h &= S'_h N_h \\ E_h &= E'_h N_h \\ I_h &= I'_h N_h \\ R_h &= R'_h N_h \\ S_m &= S'_m N_m \\ E_{m,i} &= E'_{m,i} N_m \\ I_m &= I'_m N_m \end{aligned} \tag{2.5}$$

to get the system:

$$
\begin{aligned}
\mu_h N_h \frac{dS'_h}{dT} &= \mu_h N_h - \frac{\beta_h I'_m N_m S'_h N_h}{N_h} - \mu_h S'_h N_h \\
\mu_h N_h \frac{dE'_h}{dT} &= \frac{\beta_h S'_h N_h I'_m N_m}{N_h} - (\mu_h + \sigma_h) E'_h N_h \\
\mu_h N_h \frac{dI'_h}{dT} &= \sigma_h E'_h N_h - (\mu_h + \gamma_h) I'_h N_h \\
\mu_h N_h \frac{dR'_h}{dT} &= \gamma_h I'_h N_h - \mu_h R'_h N_h
\end{aligned}
$$

$$
\begin{aligned}
\mu_h N_m \frac{dS'_m}{dT} &= N_m \mu_m - \frac{\beta_m I'_h N_h S'_m N_h}{N_h} - \mu_m S'_m N_h \\
\mu_h N_m \frac{dE'_{m,1}}{dT} &= \frac{\beta_m I'_h N_m S'_m N_h}{N_h} - (\mu_m + \rho) E'_{m,1} N_h \\
&\vdots \\
\mu_h N_m \frac{dE'_{m,i}}{dT} &= \rho E'_{m,i-1} N_h - (\mu_m + \rho) E'_{m,i} N_h \\
&\vdots \\
\mu_h N_m \frac{dI'_m}{dT} &= \rho E'_{m,n} N_h - \mu_m I'_m N_h
\end{aligned}
\tag{2.6}
$$

Divide by $\mu_h N_h$ for human equations and divide by $\mu_h N_m$ for the mosquito eqns to

get the system:

$$
\begin{aligned}
\frac{dS'_h}{dT} &= 1 - \frac{\beta_h N_m}{N_h \mu_h} I'_m S'_h - S'_h \\
\frac{dE'_h}{dT} &= \frac{\beta_h N_m}{N_h \mu_h} I'_m S'_h - \left(1 + \frac{\sigma_h}{\mu_h}\right) E'_h \\
\frac{dI'_h}{dT} &= \frac{\sigma_h}{\mu_h} E'_h - \left(1 + \frac{\gamma_h}{\mu_h}\right) I'_h \\
\frac{dR'_h}{dT} &= \frac{\gamma_h}{\mu_h} I'_h - R'_h
\end{aligned}
$$

$$
\begin{aligned}
\frac{dS'_m}{dT} &= \frac{\mu_m}{\mu_h} - \frac{\beta_m}{\mu_h} I'_h S'_m - \frac{\mu_m}{\mu_h} S'_m \\
\frac{dE'_{m,1}}{dT} &= \frac{\beta_m}{\mu_h} I'_h S'_m - \left(\frac{\mu_m}{\mu_h} + \frac{\rho}{\mu_h}\right) E'_{m,1} \\
&\vdots \\
\frac{dE'_{m,i}}{dT} &= \frac{\rho}{\mu_h} E'_{m,i-1} - \left(\frac{\mu_m}{\mu_h} + \frac{\rho}{\mu_h}\right) E'_{m,i} \\
&\vdots \\
\frac{dI'_m}{dT} &= \frac{\rho}{\mu_h} E'_{m,n} - \frac{\mu_m}{\mu_h} I'_m
\end{aligned}
\tag{2.7}
$$

Replace with non-dimensional parameters and drop the "primes"

$$\begin{aligned}
\mu &= \frac{\mu_m}{\mu_h} \\
a &= \frac{\beta_h N_m}{\mu_h N_h} \\
b &= \frac{\sigma_h}{\mu_h} \\
c &= \frac{\gamma_h}{\mu_h} \\
d &= \frac{\beta_m}{\mu_h} \\
f &= \frac{\rho}{\mu_h} = \frac{n}{\tau \mu_h}
\end{aligned} \tag{2.8}$$

$$\begin{aligned}
\frac{dS}{dT} &= 1 - aI_m S_h - S_h \\
\frac{dE_h}{dT} &= aI_m S_h - (1+b)E_h \\
\frac{dI_h}{dT} &= bE_h - (1+c)I_h \\
\frac{dR_h}{dT} &= cI_h - R_h
\end{aligned}$$

$$\begin{aligned}
\frac{dS_m}{dT} &= \mu - dI_h S_m - \mu S_m \\
\frac{dE_{m,1}}{dT} &= dI_h S_m - (\mu + f)E_{m,1} \\
&\vdots \\
\frac{dE_{m,i}}{dT} &= fE_{m,i-1} - (\mu + f)E_{m,i} \\
&\vdots \\
\frac{dI_m}{dT} &= fE_{m,n} - \mu I_m
\end{aligned} \tag{2.9}$$

2.3.3 Finding the Endemic Equilibrium

To mimic situations of endemic disease we chose to use initial conditions equivalent to the endemic steady state of the system, if temperature forcing were not considered. Here we find an analytical expression for computing the steady state which is used in the code as the initial conditions for each simulation.

$$
\begin{aligned}
0 &= 1 - aI_m S_h - S_h \\
0 &= aI_m S_h - (1+b)E_h \\
0 &= bE_h - (1+c)I_h \\
0 &= cI_h - R_h
\end{aligned}
$$

$$
\begin{aligned}
0 &= \mu - dI_h S_m - \mu S_m \\
0 &= dI_h S_m - (\mu + f)E_{m,1} \\
&\vdots \\
0 &= fE_{m,i-1} - (\mu + f)E_{m,i} \\
&\vdots \\
0 &= fE_{m,n} - \mu I_m
\end{aligned}
\tag{2.10}
$$

Begin substituting

$$
\begin{aligned}
1 &= (aI_m + 1)S_h ==> S_h = \frac{1}{aI_m + 1} \\
aI_m S_h &= \frac{(1+b)(1+c)}{bc} R_h \\
E_h &= \frac{1+c}{bc} R_h \\
I_h &= \frac{1}{c} R_h
\end{aligned}
$$

$$
\begin{aligned}
\mu &= dI_h S_m + \mu S_m ==> S_m = \frac{\mu}{dI_h + \mu} \\
dI_h S_m &= (\mu + f)E_{m,1} ==> \left(\frac{\mu + f}{f}\right)^{n-1} \frac{\mu(\mu + f)}{f} I_m \\
E_{m,1} &= \left(\frac{\mu + f}{f}\right)^{n-1} \frac{\mu}{f} I_m \\
&\vdots \\
E_{m,i} &= \left(\frac{\mu + f}{f}\right)^{n-i} \frac{\mu}{f} I_m \\
&\vdots \\
E_{m,n-3} &= \frac{\mu + f}{f} E_{m,n-2} ==> E_{m,n-3} = \left(\frac{\mu + f}{f}\right)^{3} \frac{\mu}{f} I_m \\
E_{m,n-2} &= \frac{\mu + f}{f} E_{m,n-1} ==> E_{m,n-2} = \left(\frac{\mu + f}{f}\right)^{2} \frac{\mu}{f} I_m \\
E_{m,n-1} &= \frac{\mu + f}{f} E_{m,n} ==> E_{m,n-1} = \frac{\mu + f}{f} \frac{\mu}{f} I_m \\
E_{m,n} &= \frac{\mu}{f} I_m
\end{aligned}
\tag{2.11}
$$

$$\begin{aligned}
S_h &= \frac{1}{aI_m+1} \\
R_h &= \frac{abcI_mS_h}{(1+b)(1+c)} ==> R_h = \frac{abcI_m}{(1+b)(1+c)(aI_m+1)} \\
E_h &= \frac{aI_m}{(1+b)(aI_m+1)} \\
I_h &= \frac{abI_m}{(1+b)(1+c)(1+aI_m)}
\end{aligned}$$

$$\begin{aligned}
S_m &= \frac{\mu}{dI_h+\mu} ==> S_m = \frac{\mu}{d\left(\frac{abI_m}{(1+b)(1+c)(aI_m+1)}\right)+\mu} \\
dI_hS_m &= \left(\frac{\mu+f}{f}\right)^n \mu I_m \qquad (2.12) \\
E_{m,1} &= \left(\frac{\mu}{f}+1\right)^{n-1} \frac{\mu}{f} I_m \\
&\vdots \\
E_{m,i} &= \left(\frac{1}{f}+1\right)^{n-i} \frac{\mu}{f} I_m \\
&\vdots \\
E_{m,n} &= \frac{\mu}{f} I_m
\end{aligned} \qquad (2.13)$$

Solve for I_m. Using eqn 2.12 and substituting for I_h and S_m to get:

$$\frac{dabI_m}{(1+b)(1+c)(aI_m+1)} \times \frac{\mu}{d\left(\frac{abI_m}{(1+b)(1+c)(aI_m+1)}\right)+\mu} = \left(\frac{1}{f}+1\right)^n \mu I_m \qquad (2.14)$$

$I_m = 0$ is one of the roots, which represents the disease free state.
Now assume I_m does not equal 0; then divide it out:

$$\begin{aligned} \frac{dab}{(1+b)(1+c)(aI_m+1)\left(\frac{dabI_m}{(1+b)(1+c)(aI_m+1)}+\mu\right)} &= \left(\frac{1}{f}+1\right)^n \\ (\frac{1}{f}+1)^n(dabI_m+\mu(1+b)(1+c)(aI_m+1)) &= dab \\ I_m\left(\frac{1}{f}+1\right)^n(dab+a\mu(1+b)(1+c))+\mu(1+b)(1+c)\left(\frac{1}{f}+1\right)^n &= dab \end{aligned} \tag{2.15}$$

$$I_m = \frac{dab-\mu(1+b)(1+c)\left(\frac{1}{f}+1\right)^n}{\left(\frac{1}{f}+1\right)^n[dab+a\mu(1+b)(1+c)]} \tag{2.16}$$

Note: $\mu \gg 1$; $b \gg 1$;$c \gg 1$; and $f \gg 1$ unless $\tau = \infty$ which we are not considering at this time. Therefore $1+b \approx b$; $1+c \approx c$; and $\frac{1}{f} \approx 0$.

$$I_m \approx \frac{dab-\mu bc}{dab+\mu abc} \tag{2.17}$$

Canceling the b's gives:

$$I_m \approx \frac{da-\mu c}{da+\mu ac} \tag{2.18}$$

Using the constants from table 2.1 with $\mu = \frac{1}{14}$ and $\tau = 5$ give us $I_m = 0.000422004$ Now simplify eqns 2.13 and the approximations above to get:

$$\begin{aligned} S_h &= \frac{1}{aI_m + 1} ==> S_h = 0.426069167 \\ E_h &= \frac{aI_m}{b(aI_m + 1)} ==> E_h = 0.000131034 \\ I_h &= \frac{aI_m}{c(1 + aI_m)} ==> I_h = 0.000157241 \\ R_h &= \frac{aI_m}{aI_m + 1} ==> R_h = 0.573930833 \end{aligned}$$

$$\begin{aligned} S_m &= \frac{\mu}{\left(\frac{daI_m}{c(aI_m+1)}\right) + \mu} ==> S_m = 0.999577 \\ &\vdots \\ E_{m,i} &= \frac{\mu}{f} I_m ==> E_{m,i} = \frac{\tau}{14n} \\ &\vdots \\ I_m &= .000422004 \end{aligned} \tag{2.19}$$

(note: for n> 1 => $E_{m,i} \ll I_m$)

These values are just shown for one particular case. In the matlab program all the exact values are calculated using the exact parameter for the appropriate temperature average and these values are passed to the solver as the initial conditions to begin at the endemic steady state (assuming time-invariant EIP and mortality).

2.4 R_0

The reproduction number is the average number of secondary infections due to one infection in a completely susceptibel population. R_0 can be derived by examining the disease free equilibrium. Since an $R_0 < 1$ describes the state in which the infection dies out it is a condition requiring the system to be stable. This corresponds to all eigenvalues having real parts less than zero. First we find the Jacobian (presented in table 2.2) of the system of equations presented in eqns 2.3 and 2.4.

$$R_0 = \frac{\beta_h \beta_m \sigma_h N_m}{\mu_m N_h (\gamma_h + \mu_h)(\sigma_h + \mu_h)\left(1 + \frac{\mu_m \tau}{n}\right)^n} \tag{2.20}$$

The disease free state requires all populations are equal to zero excluding the susceptible populations (table 2.3).

Table 2.2: Jacobian of system using eqn.2.3 and 2.4

	∂S_h	∂E_h	∂I_h	∂R_h	∂S_m	$\partial E_{m,1}$	$\partial E_{m,2}$	$\cdots$	$\partial E_{m,n-1}$	$\partial E_{m,n}$	∂I_m
$\frac{dS_h}{dt}$	$-\left(\frac{\beta_h I_m}{N_h} - \mu_h\right)$	0	0	0	0	0	0	$\cdots$	0	0	$\frac{-\beta_h S_h}{N_h}$
$\frac{dE_h}{dt}$	$\frac{\beta_h I_m}{N_h}$	$-(\mu_h + \sigma_h)$	0	0	0	0	0	$\cdots$	0	0	$\frac{\beta_h S_h}{N_h}$
$\frac{dI_h}{dt}$	0	σ_h	$-(\mu_h + \gamma_h)$	0	0	0	0	$\cdots$	0	0	0
$\frac{dR_h}{dt}$	0	0	γ_h	$-\mu_h$	0	0	0	$\cdots$	0	0	0
$\frac{dS_m}{dt}$	0	0	$\frac{-\beta_m S_m}{N_h}$	0	$-\left(\frac{\beta_m I_h}{N_h} + \mu_m\right)$	0	0	$\cdots$	0	0	0
$\frac{dE_{m,1}}{dt}$	0	0	$\frac{\beta_m S_m}{N_h}$	0	$\frac{\beta_m I_h}{N_h}$	$-(\mu_m + \rho)$	0	$\cdots$	0	0	0
$\frac{dE_{m,2}}{dt}$	0	0	0	0	0	ρ	$-(\mu_m + \rho)$	$\cdots$	0	0	0
$\vdots$	0	0	0	0	0	0	$\ddots$	$\ddots$	0	0	0
$\frac{dE_{m,n-1}}{dt}$	0	0	0	0	0	0	0	$\ddots$	$-(\mu_m + \rho)$	0	0
$\frac{dE_{m,n}}{dt}$	0	0	0	0	0	0	0	$\cdots$	ρ	$-(\mu_m + \rho)$	0
$\frac{dI_m}{dt}$	0	0	0	0	0	0	0	$\cdots$	0	ρ	$-\mu_m$

Table 2.3: Jacobian presented in table 2.2 evaluated ath the disease free state equilibrium where R_1 is a (n-4)x(n-4) bidiagonal matrix with diagonal $-(\mu_m + \rho)$ and sub-diagonal ρ. R_2 is a column vector of length n-4 of zeros except $R_2(1) = \rho$; R_3 is a zero row vector of length n-4 except $R_3(n-4) = \rho$. Z_1 is a 7x(n-4) zero matrix, Z_2 is a (n-4)x6 zero matrix, Z_3 is a (n-4)x3 zero matrix, and Z_4 is a 2x(n-4) zero matrix.

	∂S_h	∂E_h	∂I_h	∂R_h	∂S_m	$\partial E_{m,1}$	$\partial E_{m,2}$	$\cdots$	$\partial E_{m,n-1}$	$\partial E_{m,n}$	∂I_m
$\frac{dS_h}{dt}$	$-\mu_h$	0	0	0	0	0	0		0	0	$\frac{-\beta_h S_h}{N_h}$
$\frac{dE_h}{dt}$	0	$-(\mu_h + \sigma_h)$	0	0	0	0	0		0	0	$\frac{\beta_h S_h}{N_h}$
$\frac{dI_h}{dt}$	0	σ_h	$-(\mu_h + \gamma_h)$	0	0	0	0		0	0	0
$\frac{dR_h}{dt}$	0	0	γ_h	$-\mu_h$	0	0	0	Z_1	0	0	0
$\frac{dS_m}{dt}$	0	0	$\frac{-\beta_m S_m}{N_h}$	0	-μ_m	0	0		0	0	0
$\frac{dE_{m,1}}{dt}$	0	0	$\frac{\beta_m S_m}{N_h}$	0	0	$-(\mu_m + \rho)$	0		0	0	0
$\frac{dE_{m,2}}{dt}$	0	0	0	0	0	ρ	$-(\mu_m + \rho)$		0	0	0
$\vdots$			Z_2				R_2	R_1		Z_3	
$\frac{dE_{m,n-1}}{dt}$	0	0	0	0	0	0	0	R_3	$-(\mu_m + \rho)$	0	0
$\frac{dE_{m,n}}{dt}$	0	0	0	0	0	0	0	Z_4	ρ	$-(\mu_m + \rho)$	0
$\frac{dI_m}{dt}$	0	0	0	0	0	0	0		0	ρ	$-\mu_m$

We are looking for the eigenvalues so we must find the determinant of the matrix J.

$$J = \begin{pmatrix}
-\mu_h - \lambda & 0 & 0 & 0 & 0 & 0 & 0 & \cdots & 0 & 0 & \frac{-\beta_h S_h}{N_h} \\
0 & -\mu_h - \sigma_h - \lambda & 0 & 0 & 0 & 0 & 0 & \cdots & 0 & 0 & \frac{\beta_h S_h}{N_h} \\
0 & \sigma_h & -\mu_h - \gamma_h - \lambda & 0 & 0 & 0 & 0 & \cdots & 0 & 0 & 0 \\
0 & 0 & \gamma_h & -\mu_h - \lambda & 0 & 0 & 0 & \cdots & 0 & 0 & 0 \\
0 & 0 & \frac{-\beta_m S_m}{N_h} & 0 & -\mu_m - \lambda & 0 & 0 & \cdots & 0 & 0 & 0 \\
0 & 0 & \frac{\beta_m S_m}{N_h} & 0 & 0 & A & 0 & \cdots & 0 & 0 & 0 \\
0 & 0 & 0 & 0 & 0 & \rho & A & & 0 & 0 & 0 \\
 & & Z_2 & & & & R_2 & R_1 - \lambda I & 0 & 0 & 0 \\
0 & 0 & 0 & 0 & 0 & 0 & 0 & R_3 & A & 0 & 0 \\
0 & 0 & 0 & 0 & 0 & 0 & 0 & Z_4 & \rho & A & 0 \\
0 & 0 & 0 & 0 & 0 & 0 & 0 & \cdots & 0 & \rho & -\mu_m - \lambda
\end{pmatrix}$$

For space concerns allow A=$-(\mu_m+\rho+\lambda)$.

After a little algebraic tweaking one gets the lower triangular matrix J_1 whose determinant is simply the product of the diagonal terms. Where, again, A $=-(\mu_m + \rho + \lambda)$ and

$$B = -\left[\mu_h + \sigma_h - \frac{S_h S_m \beta_h \beta_m \sigma_h \rho^n}{N_h^2(\mu_h + \gamma_h)(\mu_m + \lambda)(\mu_m + \rho)^n}\right] \tag{2.21}$$

$$
J_1 = \begin{pmatrix}
-\mu_h - \lambda & 0 & 0 & 0 & 0 & 0 & 0 & \cdots & 0 & 0 & 0 \\
0 & B & 0 & 0 & 0 & 0 & 0 & \cdots & 0 & 0 & 0 \\
0 & \sigma_h & -\mu_h - \gamma_h - \lambda & 0 & 0 & 0 & 0 & \cdots & 0 & 0 & 0 \\
0 & 0 & \gamma_h & -\mu_h - \lambda & 0 & 0 & 0 & \cdots & 0 & 0 & 0 \\
0 & 0 & \frac{-\beta_m S_m}{N_h} & 0 & -\mu_m - \lambda & 0 & 0 & \cdots & 0 & 0 & 0 \\
0 & 0 & \frac{\beta_m S_m}{N_h} & 0 & 0 & A & 0 & \cdots & 0 & 0 & 0 \\
0 & 0 & 0 & 0 & 0 & \rho & A & & 0 & 0 & 0 \\
 & & Z_2 & & & & R_2 & R_1 - \lambda I & 0 & 0 & 0 \\
0 & 0 & 0 & 0 & 0 & 0 & 0 & R_3 & A & 0 & 0 \\
0 & 0 & 0 & 0 & 0 & 0 & 0 & Z_4 & \rho & A & 0 \\
0 & 0 & 0 & 0 & 0 & 0 & 0 & \cdots & 0 & \rho & -\mu_m - \lambda
\end{pmatrix}
$$

which results in the n+5 degree characteristic polynomial:

$$0 = (-1)^n \left[(\mu_m + \lambda)(\mu_h + \sigma_h) - \frac{\beta_h \beta_m S_h S_m \sigma_h \rho^n}{N_h^2 (\mu_h + \gamma_h)(\mu_m + \rho)^n} \right] (\mu_h + \lambda)(\mu_h + \gamma_h + \lambda) \\ (\mu_h + \lambda)(\mu_m + \lambda)(\mu_m + \rho + \lambda)^n \tag{2.22}$$

In our case with n=10 this simplifies to:

$$0 = \left[(\mu_m + \lambda)(\mu_h + \sigma_h) - \frac{\beta_h \beta_m S_h S_m \sigma_h \rho^{10}}{N_h^2 (\mu_h + \gamma_h)(\mu_m + \rho)^{10}} \right] (\mu_h + \lambda)(\mu_h + \gamma_h + \lambda) \\ (\mu_h + \lambda)(\mu_m + \lambda)(\mu_m + \rho + \lambda)^{10} \tag{2.23}$$

For stability, we require all $\lambda < 0$ which is trivial for most of the terms as our parameters are all positive values. There is only one term which remains to examine.

$$0 = (\mu_m + \lambda)(\mu_h + \sigma_h) - \frac{\beta_h \beta_m S_h S_m \sigma_h \rho^{10}}{N_h^2 (\mu_h + \gamma_h)(\mu_m + \rho)^{10}} \tag{2.24}$$

This simplifies to:

$$\lambda = -\mu_m + \frac{\beta_h \beta_m S_h S_m \sigma_h \rho^{10}}{N_h^2 (\mu_h + \gamma_h)(\mu_h + \sigma_h)(\mu_m + \rho)^{10}} \tag{2.25}$$

but as it is the disease free state, $S_m = N_m$ and $S_h = N_h$. Also note that because $\rho = \frac{n}{\tau}$

$$\left(\frac{\rho}{\mu_m + \rho} \right)^{10} = \left(\frac{1}{\frac{\mu_m}{\rho} + 1} \right)^{10} = \left(\frac{1}{\frac{\mu_m \tau}{10} + 1} \right)^{10} \tag{2.26}$$

and so equation 2.25 simplifies to

$$\lambda = -\mu_m + \frac{\beta_h \beta_m N_m \sigma_h}{N_h (\mu_h + \gamma_h)(\mu_h + \sigma_h)(\frac{\mu_m \tau}{10} + 1)^{10}} < 0 \tag{2.27}$$

For our system more generally,

$$R_0 = \frac{\beta_h \beta_m \sigma_h N_m}{\mu_m N_h (\gamma_h + \mu_h)(\sigma_h + \mu_h) \left(\frac{\mu_m \tau}{n} + 1 \right)^n} < 1 \tag{2.28}$$

Chapter 3

Results

Given the model as described, we will first look at R_0 as a function of temperature. We will then look at the simulations of the vector and human populations using various temperatures, temperature ranges, and means of varying temperature. A presentation of the different EIP data sets and the resulting temperature-dependent functions is accompanied by an examination of the potential persistence given multiple mortality rates. Results are given of the addition of a time dependent mortality function. Differing initial conditions are presented. This is followed by examining the effects of annual and diurnal forcing with EIP only dependence and then mortality is also temperature-dependent. The addition of a minimum population cut-off is also examined.

3.1 R_0 as a Function of Temperature

R_0 as calculated with EIP only temperature dependence, assuming a mean yearly temperature of 29.4°C and multiple temperature ranges, is shown in Fig. 3.1. It begins mid-spring (day 0) and is plotted over the course of the year. The R_0 is so

high because of the mortality rate used, $\mu = \frac{1}{27}$, which has increased the R_0 to values outside those observed in the field. This μ was chosen so that figures 3.1, 3.2, 3.3, and 3.4 could be compared directly given that the mortality rate function used by Yang gives a survival length of approximately 27 days at 29.4°C. As one can see, R_0 increases entering in to the summer (day 45) and plateaus if the range is large enough. R_0 then begins to decrease as it approaches fall (day 136) and then drops, drastically or moderately, depending upon the temperature range. This drop is due to the increase in length of the EIP during the colder winter months. Considering only changes to EIP, R_0 can be increased slightly or reduced greatly with a large enough temperature range.

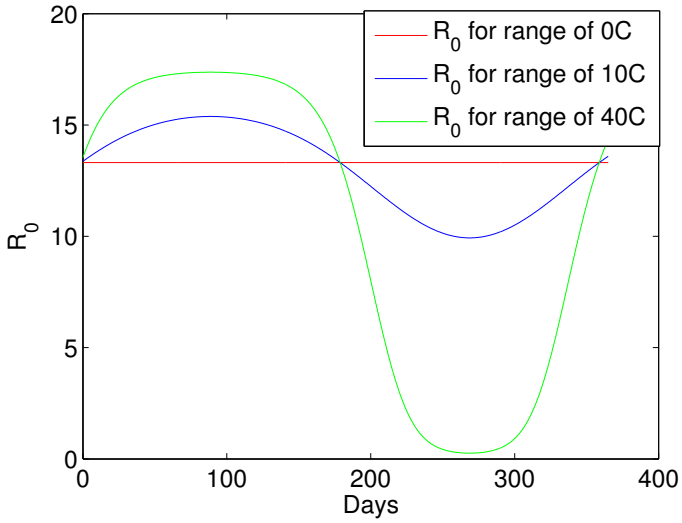

Figure 3.1: R_0 with an annual cycle considering EIP only for 29.4°C

The same parameters used in Fig. 3.1 are used to obtain the plot of Fig. 3.2 except now the mortality rate is not constant at $\frac{1}{27}$ (1/days), but is temperature dependent. One observes two drops in R_0; the first is during the summer when the increase in temperature leads to a higher mortality rate. The larger the range, the greater the

increase and thus a greater reduction in the R_0. The second drop off is again due to the lengthening of the EIP, but is compounded by the increase in the death rate at lower temperatures.

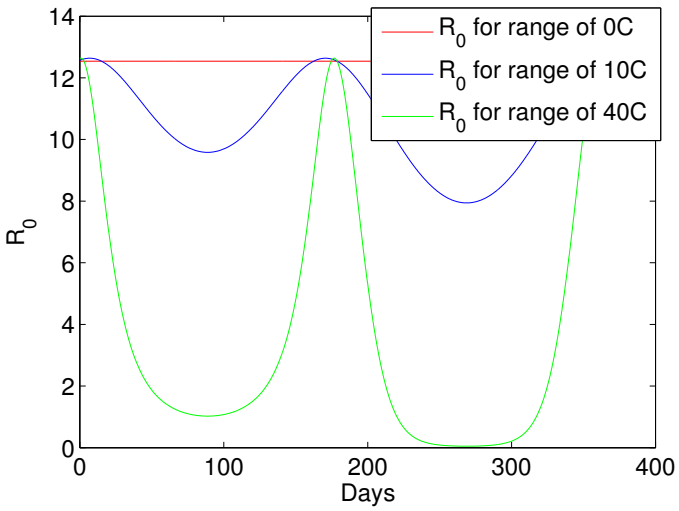

Figure 3.2: R_0 with an annual cycle considering EIP and vector mortality for 29.4°C

In Fig. 3.3, R_0 is calculated with EIP only temperature-dependence and a mean yearly temperature of 29.4°C with multiple temperature ranges, with a diurnal temperature fluctuation of 9.44°C. It also begins in the spring and is plotted over the course of a year. Here R_0 is constantly changing, even with no yearly change in temperature the daily fluctuation forces R_0 to vary between 6.9 and 16.3. For each of the temperature ranges it also appears that they follow a similar pattern to what was observed in Fig. 3.1 except that each varies about this pattern with different envelopes. In the summer with a large temperature range, the resulting R_0 is restricted to a very high value (16.71-17.57), but in the winter it decreases while the range of R_0 values is greatly expanded (.00058-4.27). With a range of 10°C, R_0 has a greatly increased envelope of values which do contract in the summer (11.07-16.95) as compared to the winter (2.76-14.88) but not as severely as the large temperature

range.

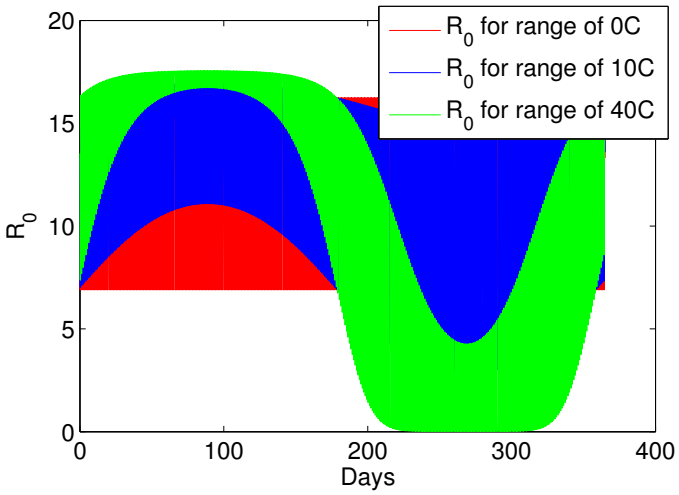

Figure 3.3: R_0 with an annual and diurnal cycle considering only EIP for 29.4°C

Fig. 3.4 uses the same settings as Fig. 3.3, except that vector mortality is now temperature dependent. Where previously, the EIP only temperature-dependence with annual and diurnal forcing showed some similarity, here it is absent. With the incorporation of mortality and diurnal temperature changes, no annual variation and only daily temperature change results in R_0 values between 4.04 and 12.34. In the summer, a temperature range of 10°C results in values from 2.56 to 9.74; this range is expanded in the winter to between .93 and 11.78. The range of 40°C has a range of values between .41 and 3.54 during the summer and .000006 to 1.80 during the winter. The additional maxima and minima are due to the interaction of shortened EIP with high mortality rates and short time exposures to extreme temperatures.

It is very clear that given any variation in a region's temperature, whether simply annually or daily, the resulting R_0 is not constant. A variable R_0 implies a varying ability of the pathogen to persist as well as a variation in the strength to which it will persist. Therefore, if R_0 is less than one for long enough, extinction will occur

where one might expect persistence given its average value.

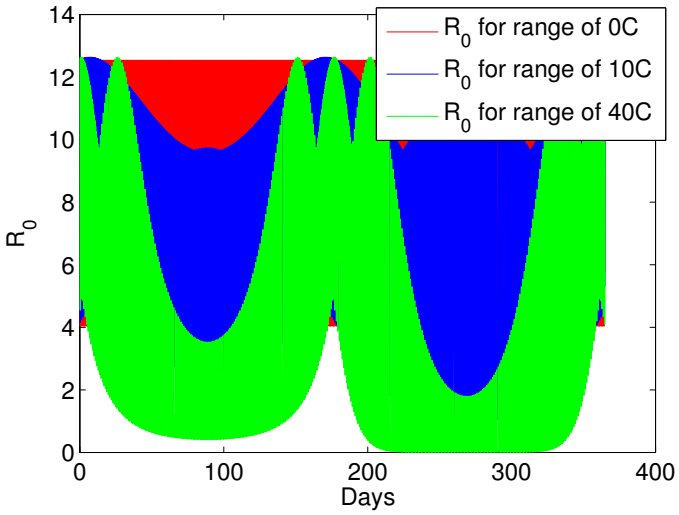

Figure 3.4: R_0 with an annual and diurnal cycle considering EIP and vector mortality for 29.4°C

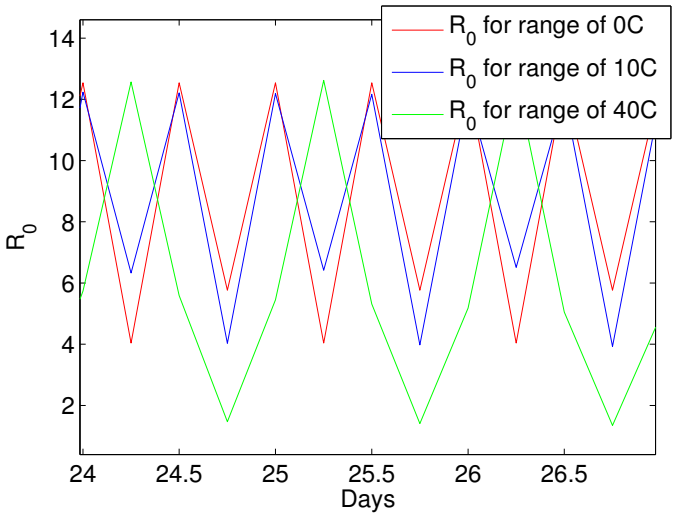

Figure 3.5: R_0 with an annual and diurnal cycle considering EIP and vector mortality for 29.4°C zoomed in to days 24-27

3.2 Model Simulations

3.2.1 Time Series and Spectral Analysis

Matlab's ode45 function was used to solve the system described in section 2.3.2. First we consider the effects of temperature-dependent EIP as well as vector mortality given a constant temperature of 26.7°C and 32.2°C with no temperature forcing. The population levels are shown in Fig. 3.6. One can see the disease persists at high levels for both temperatures.

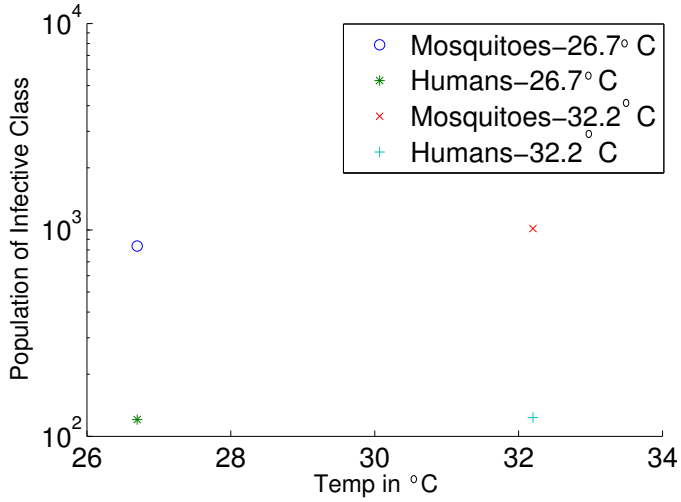

Figure 3.6: Population levels of the infected class for the vector and host populations when no temperature forcing is considered for temperatures 26.7°C and 32.2°C.

An example of annual temperature forcing is shown in Fig. 3.7. Each simulation has a temperature range of 11.02°C such that in Fig. 3.7a the temperature varies between 21.14°C and 32.26°C and in Fig. 3.7b it varies between 26.64°C and 37.76°C. The temperature range of 11.02°C was chosen as it displays the potential time series results most clearly for all the experiments attempted. There is clearly now an annual peak of incidence, what is interesting is that in (a) this peak is in the fall whereas in

(b) its peak is in the spring. Each goes through a trough after three or five years but the human infected population of (a) reaches a minimum of 1.092 while in (b) the human population has a minimum of 1.08E-8 which could indicate, given a stochastic model, that the infection would not recover and would instead go extinct.

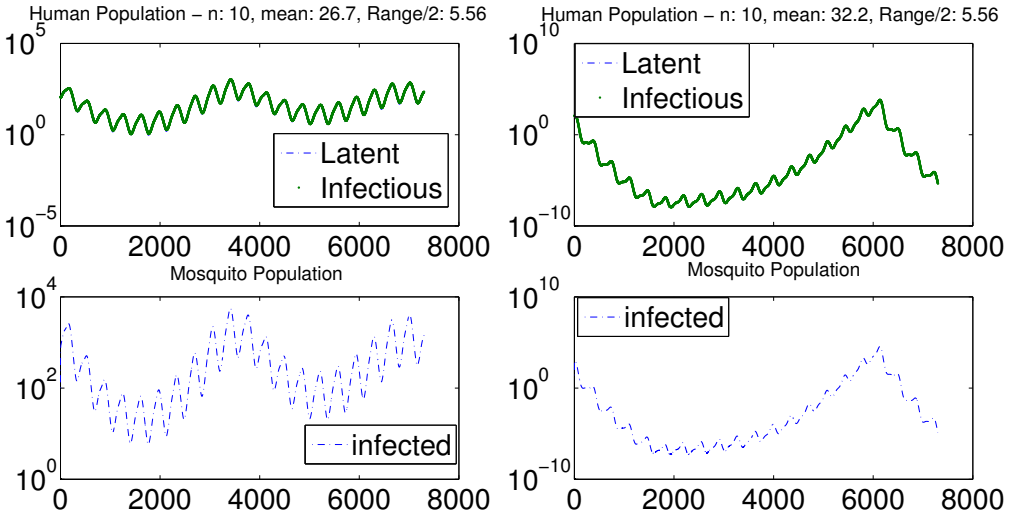

(a) 26.7°C (b) 32.2°C

Figure 3.7: Example of time series with temperature forcing on an annual scale with a temperature range of 11.02°C

Assuming a constant yearly temperature, but daily temperatures that fluctuate about that temperature with a range of 9.44°C introduces a third set of dynamics. There are no longer yearly cycles, which is expected, but each simulation has a dominant period representing a large epidemic every 7 years (a) and every 11 years (b). Again 26.7°C and 32.2°C go through troughs in the infective population but minima are quite different, 78.6 and .00079 respectively.

In Fig. 3.9 we now have both annual and diurnal temperature fluctuations. For (a), on the hottest day temperatures would reach 36.98°C and on the coldest night temperatures would drop to 16.42°C. Likewise, in (b), temperatures get as high as

42.48°C and as low as 21.92°C. The annual cycles are again very evident in both models with 26.7°C again showing another multi-year cycle of approximately 11 years. It does go through a trough again after about three years but never has a human infectious population below 1.01 and then the disease recovers to have a maximum infectious population of over 780. 32.2°C on the other hand, experiences three years of the human infectious population being no larger than 4.4E-8. Under these conditions it is unlikely that the disease would be able to persist to again reach an infectious population greater than one as is indicated after nearly 20 years.

The time series of the human infectious population was then subjected to spectral analysis using Matlab's fft function after which the spectral peaks with the two largest amplitudes were used to determine the two dominant periods of the time series. The mean value of the signal was subtracted out in order that the zero-frequency would be ignored and the standard deviation of the signal was divided out such that the amplitudes of the significant frequencies could be compared. The total length of each of the time series is 20 years so any period that is greater than half of this length (ten years) is not reliable given the length of data sampling. The results of the spectral analysis for the time series with daily temperature forcing but no yearly forcing are shown in Fig. 3.10. For 26.7°C and 32.2°C the maximum peaks are periods of 7.18 years and 11.97 years respectively as was discussed previously but 11.97 years can not be taken as a reliable period as the signal is only 20 years in length. Given the structure of the spectral analysis results there is little meaning in the secondary periods (13.81 years and 4.38 years for (a) and (b) respectively). However, when looking at Fig. 3.11, the spectral analysis results of Fig. 3.7a which is a mean temperature of 26.7°C with annual forcing in the range of 11.12°C, one can see a different result and interpretation. The peak periods are 8.16 years and .99 years, both of which are evident in the time series plot. Every year there is a cycle of increase and decrease in incidence from the temperature change and approximately every eight years there is a larger epidemic. This longer period which results in a

sizeable epidemic is an intrinsic aspect of the pathogen's biology and is approximated by $2\pi\sqrt{\frac{1}{\mu(R_0-1)(\mu+\gamma)}}$ [22] for directly transmitted diseases. In our case it is generalized to $2\pi\sqrt{\frac{LG}{R_0-1}}$ where L is a function of the lifespan of the human host and G is a function of the generation time of the pathogen.

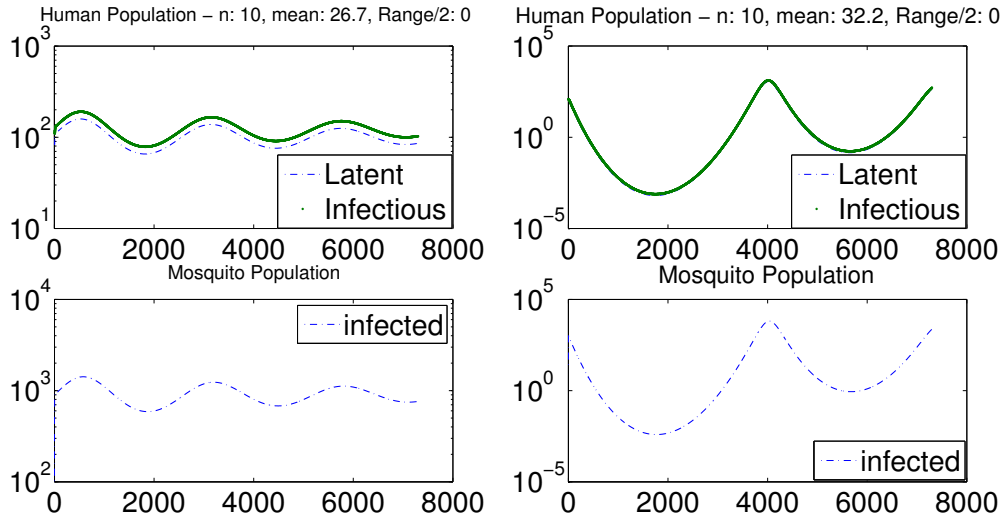

(a) 26.7°C (b) 32.2°C

Figure 3.8: Example of time series with temperature forcing on a daily scale with a temperature range of 9.44°C

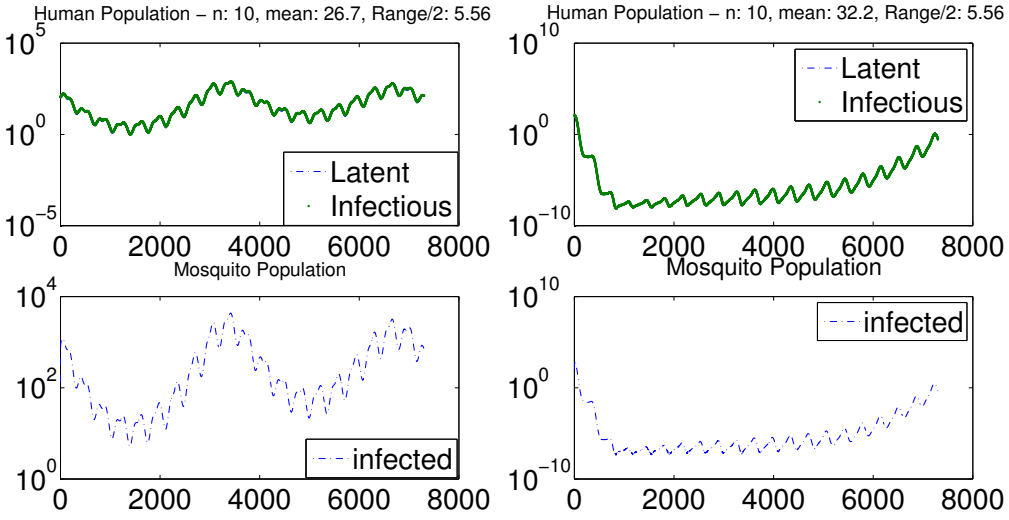

(a) 26.7°C (b) 32.2°C

Figure 3.9: Example of time series with temperature forcing on a daily scale with a temperature range of 4.72°C as well as annual forcing with a temperature range of 11.02°C

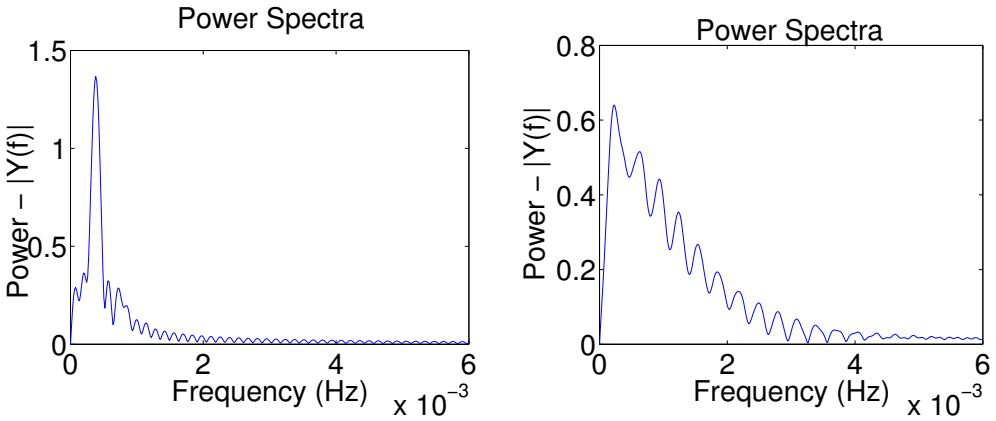

(a) 26.7°C (b) 32.2°C

Figure 3.10: Example of spectral analysis results from the time series of Fig. 3.8. Maximum peaks give a period of 7.18 years Fig. (a) and 11.97 years Fig. (b) but 11.97>10 which is half of the time series total length. Secondary peaks give period of 13.81 Fig. (a) and 4.38 years Fig. (b) with 13.81>10 so again this period can not be taken as a reliable period.

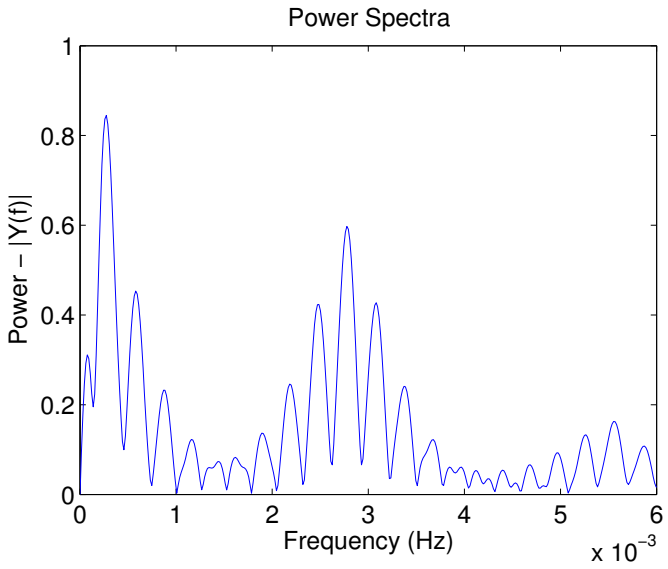

Figure 3.11: Example of spectral analysis results from the time series of annual temperature forcing with a mean temperature of 26.7°C a temperature range of 11.12°C. Maximum peak gives a period of 8.16 years and the secondary peak gives a period of .99 years.

3.3 Colorplots of Incidence Based upon Specific EIP Data Sets

In this section, the last ten years of the observed infective human population was averaged and this was then used to determine the percentage of infectives out of the total human population for each time series for mean temperatures of [21.1, 23.9, 26.7, 29.4, 32.2, 35.0, 37.8] each with temperature ranges of [2.22, 4.44, 6.66, 8.88, 11.12, 13.34, 15.56, 17.78, 20.0, 22.2]. The colorplots represent this percentage for each of the means and temperature range to attempt to see consistent persistence or extinction of the disease. The mortality rate is held constant so that one can look at the effects of only the temperature-dependent EIP. The EIP function is described in table 2.1 and corresponds to the appropriate EIP data set. The leftmost figure has a mortality rate of $\frac{1}{27}$, this is the average of Yang's function for temperatures 21.1-37.8. The center figure has a mortality rate of $\frac{1}{14}$ which is biologically reasonable given the wide range of temperatures. The rightmost figure is a plot of the data points and the line of best fit found for the particular data set used.

Using the data given by McLean *et al*., one can see that persistence is possible in all temperature ranges for both mortality rates (see Fig. 3.12). There may be a slight decline for a mean temperature of 21.1°C and the largest range, but even this is not zero. One can also observe that a much larger percentage of the population is infective over the entire range of temperatures in Fig. (a) versus Fig. (b) which is due entirely to the difference in vector mortality. The mosquito lives longer in (a) and is able to take more infective bites over the course of its lifetime and this results in higher transmission. The temperature at which the EIP is the same as the vector survival is approximately 16.11°C and 24.37°C for (a) and (b) respectively which means that the variation in temperature may in some way have a rescue effect for the mean temperatures of 21.1°C and 23.9°C when the survival time is 14 days.

The other possibility is that with the EIP and mortality rate being the same length of time, transmission is reduced but not impossible. The dynamics of temperature ranges here "on the boundary" would probably benefit from a stochastic model.

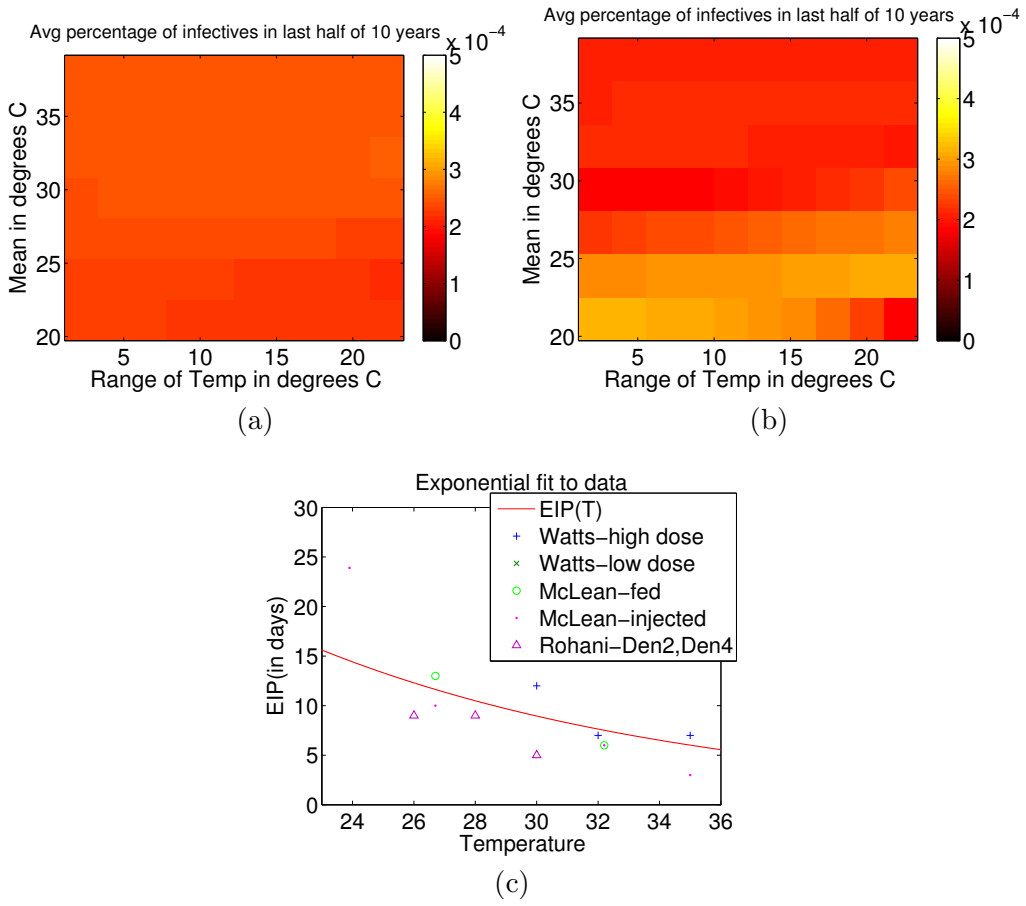

Figure 3.12: Color plot with the average of the last half of the time series for EIP with a fit based on McLean's Feeding data only with annual temperature forcing starting mid-spring. (a)Colorplot of incidence with mosquito survival set at 27 days. (b)Colorplot of incidence with mosquito survival set at 14 days. (c) Exponential fit: $97.177e^{-.0795T}$

The results using data from Rohani *et al.* are quite similar, which is not surprising given that the two exponential functions are similar. Fig. 3.13 shows persistence is possible in all temperature ranges and incidence is higher given a lower vector

mortality. Given this function, the temperature at which the EIP matches the length of survival is approximately 15.386°C for 27 day survival and 21.915°C given 14 days of survival. Given the range of temperatures examined, there would be no hinderance to persistence at these EIP and mortality rates.

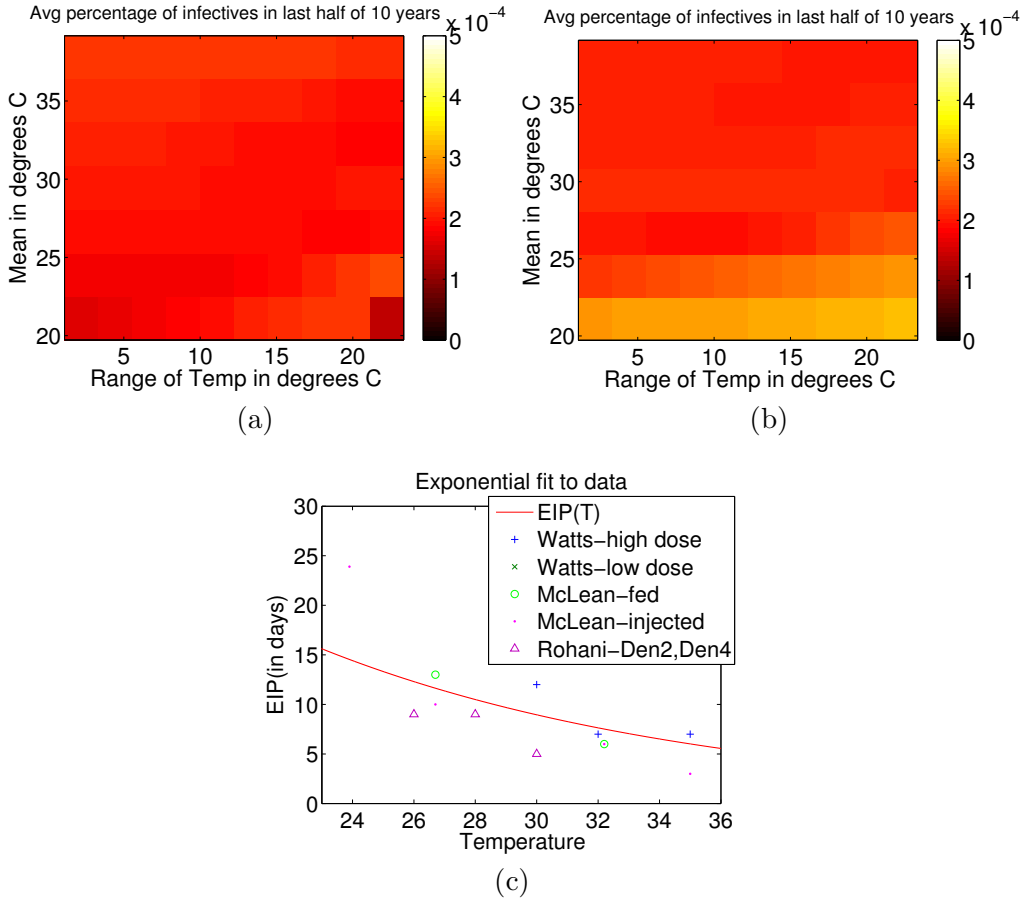

Figure 3.13: Color plot with the average of the last half of the time series for EIP with a fit based on Rohani's data with only annual temperature forcing starting mid-spring. (a) Colorplot of incidence with mosquito survival set at 27 days. (b) Colorplot of incidence with mosquito survival set at 14 days. (c) Exponential fit: $126.9373e^{-0.1006T}$.

With the data from Watts we see the potential for different results (see Fig. 3.14), given a survival time of 27 days the temperature at which the EIP matches this is still

low at 23.075°C giving ample temperature ranges at which dengue could persist. This is clear in the presence of dengue for all temperature ranges in Fig. 3.14. However, the temperature when the mortality rate is $\frac{1}{14}$ is increased to 28.266°C which mirrors the observed extinction at mean temperatures of 21.1 and 23.9 and with a large enough range given a mean temperature of 26.7 in Fig. 3.14b.

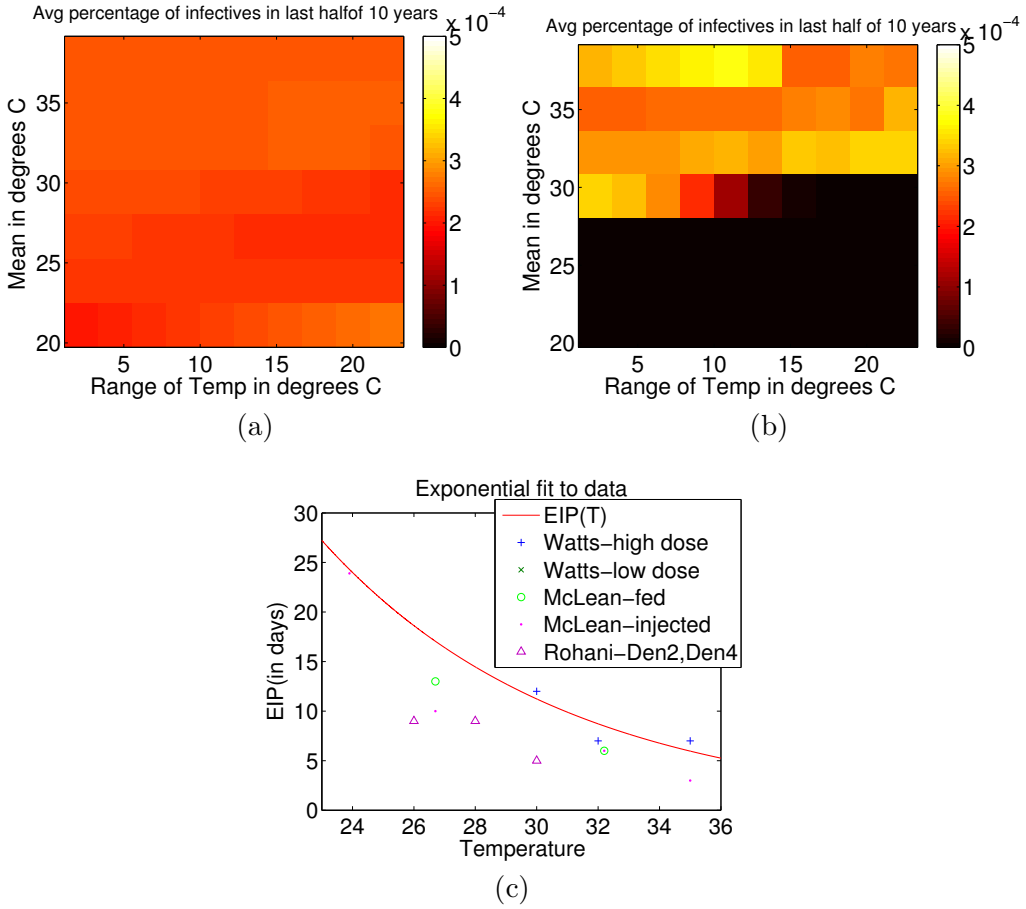

Figure 3.14: Color plot with the average of the last half of the time series for EIP with a fit based on Watts' data only with annual temperature forcing starting mid-spring. (a)Colorplot of incidence with mosquito survival set at 27 days. (b)Colorplot of incidence with mosquito survival set at 14 days. (c)Exponential fit: $500.1015e^{-.1265T}$.

Fig. 3.15 shows the EIP function that was fit to multiple data sets and is the function that is used hereafter. Given a survival time of 27 days this is matched by the

EIP at a temperature of approximately 26.165°C; a survival of 14 days corresponds to 28.672°C. Here, (Fig. 3.15a) even with a long survival time we see persistence is not possible for the 21.1°C mean temperature case and is only possible for small ranges of temperature around 23.9°C. Too large of a range seems to force the EIP to be too long for an extended period of time such that incidence can not be sustained. A shortened survival time cuts off persistence even more as seen in Fig. 3.15b. For mean temperatures of 21.1, 23.9, and 26.7°C there is no persistence, and not until 29.4°C do we see sustained incidence and for a range of temperatures.

Using the EIP function given by multiple data sets in conjunction with the temperature dependent mortality function with annual temperature forcing is shown in Fig. 3.16. Persistence is no longer possible in all higher temperatures for all ranges. Instead as the temperature increases the temperature ranges that show persistence dwindle.

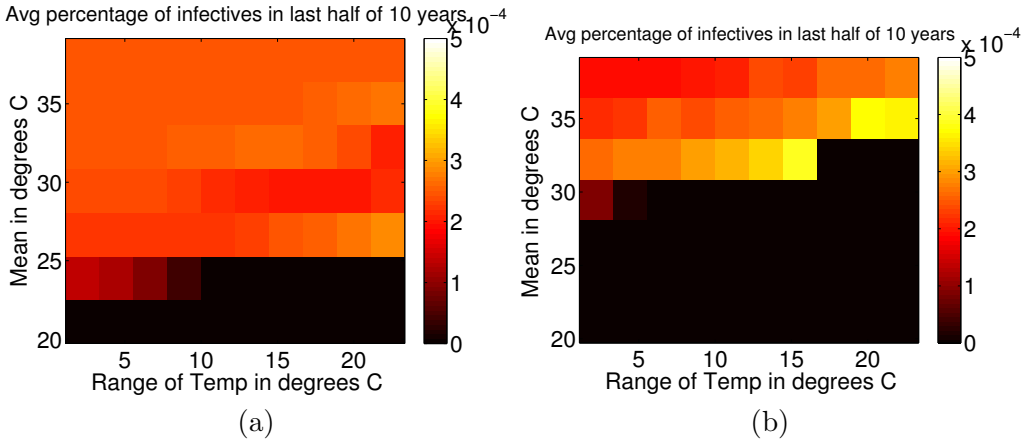

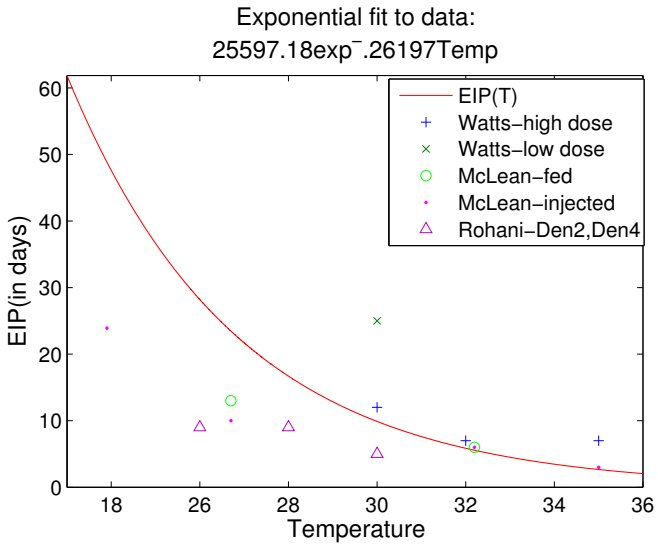

Figure 3.15: Color plot with the average of the last half of the time series for EIP with an exponential function from multiple data sets using only annual temperature forcing starting mid-spring. (a) Colorplot of incidence with mosquito survival set at 27 days. (b) Colorplot of incidence with mosquito survival set at 14 days. (c) Exponential fit: $25597.18e^{-.26197T}$.

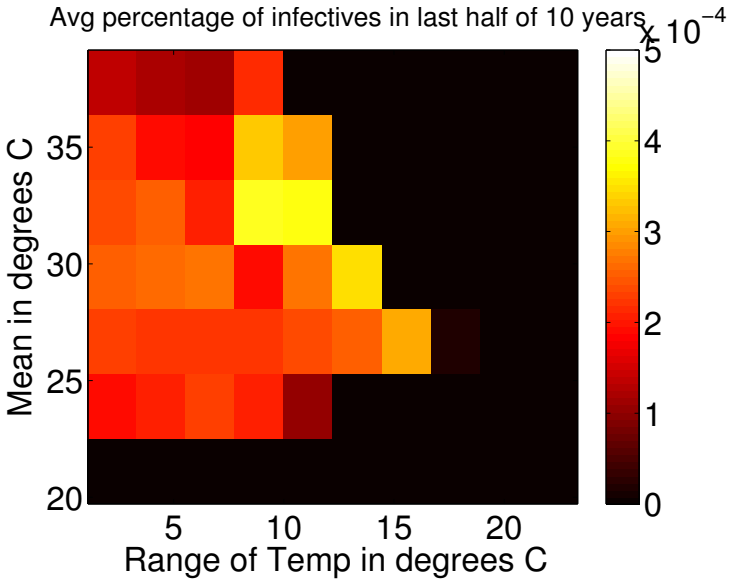

Figure 3.16: Color plot with the average of the last half of the time series for EIP and vector mortality with annual temperature forcing.

3.4 Effects of Varying Initial Conditions

Since the initial conditions of time dependent ordinary differential equations can have profound influence upon the resulting solution, four time periods representing the four seasons were used to examine the differences when the model is begun mid-season (Fig. 3.17). Summer, fall, and winter give very similar results only differing in presence of disease for mean temperatures of 21.1°C and 37.8°C with two ranges each and the strength of incidence given a mean of 35.0°C and a range of 5.56°C. A start time in the spring, however, is different in that it allows all the higher mean temperatures that had persistence in any of the other three models to persist and persist at a higher percentage, the mean temperature of 23.9°C loses persistence for any range about the mean greater than 11.12 °C and has no persistence for 21.1°C which is a departure from the other three initial conditions. This is somewhat surprising in that given a reduction in the allowed range for lower temperature means one would expect a winter start to also have a reduction in the lower means but this is not the case.

Looking at the plot of R_0 as seen in Fig. 3.18, given a large enough range, the R_0 drops both mid-summer and through the winter. It is not surprising that large temperature ranges do not persist for this low mean temperature; what is surprising is that the other three seasons *do* allow it to persist. An example is shown of a timeseries that persists given a summer initial condition but does not persist for the spring (see Fig. 3.19). A spring start begins with more mosquitoes and humans that are infectious but it decays at a faster rate and to a much lower value. For consistency we used an initial start in the spring for all simulations excluding these plots as it was the most limited in giving persistence and thus may be prone to under-prediction in the lower temperatures with large ranges.

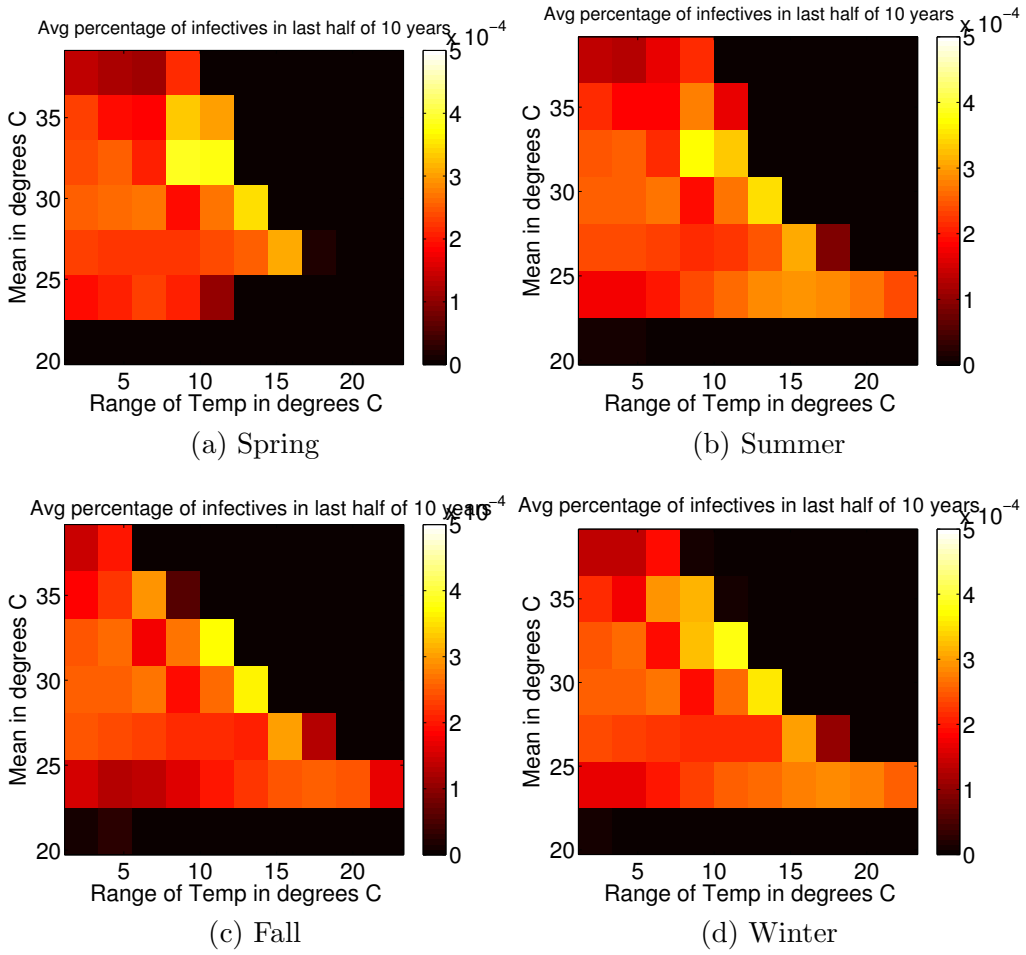

Figure 3.17: Color plot with the average of the last half of the time series for EIP and vector mortality with annual temperature forcing starting in different seasons: (a) spring, (b) summer, (c) fall, (d) winter.

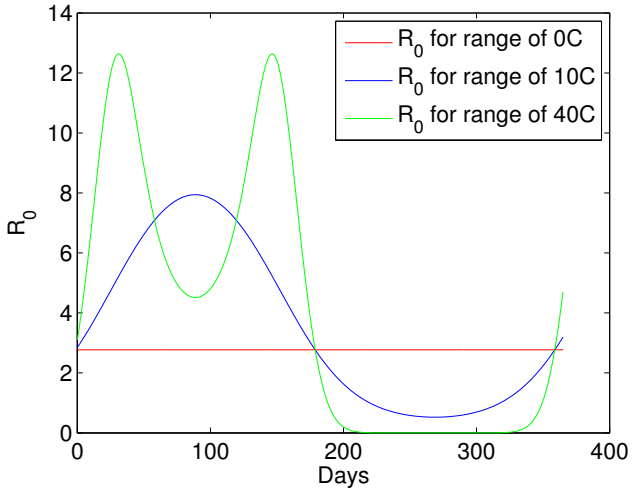

Figure 3.18: R_0 for 23.9°C with EIP and vector mortality given annual forcing.

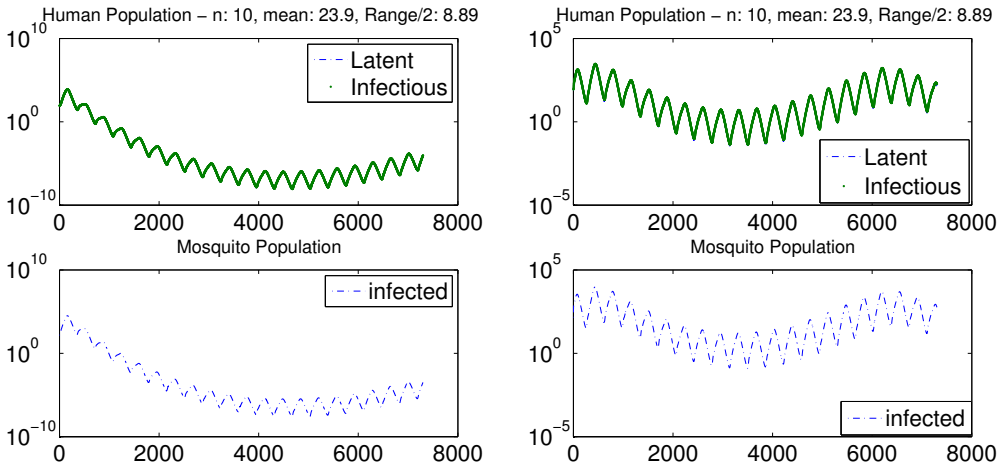

(a) Spring (b) Summer

Figure 3.19: Time series of spring and summer with 23.9°C and a range of 17.72°C with differing persistence based on the season in which the simulation is initiated.

3.5 Colorplots with Annual and Diurnal Temperature Forcing

An annual temperature forcing with a constant mortality rate of $\frac{1}{27}$ gave persistence for all mean tempertures greater than or equal to 26.7°C and for a limited range of temperatures with a mean of 23.9°C (see Fig. 3.15a). When a daily temperature range of 9.44°C is also added (Fig. 3.20) we see that incidence in the lower temperatures decreases, and only an annual range of 11.12°C with a mean of 23.9°C has persistence but the level of incidence is greatly reduced.

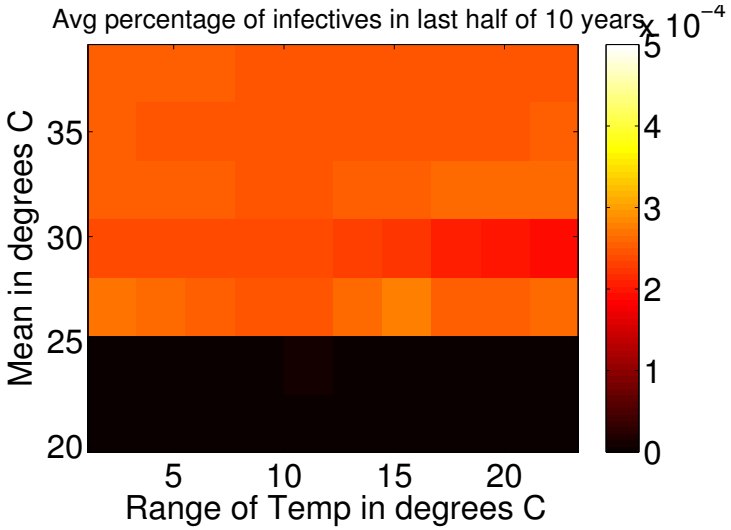

Figure 3.20: Color plot with the average of the last half of the time series for EIP only with annual temperature forcing with a diurnal forcing with a temperature range of 9.44°C starting mid-spring

When EIP as well as vector mortality are allowed to vary with diurnal forcing the range of temperatures that allow for persistence is greatly changed (Fig. 3.20 versus Fig. 3.21). Lower temperatures show persistence and many of the higher temperatures can no longer sustain the disease. When the temperature gets too

high the mortality rate increases dramatically and so although the EIP is short, the mosquitoes are dying too quickly for the disease to reach the salivary glands and the disease dies out, this was also shown in the reduction of R_0 over the winter as well as summer months in Fig. 3.3.

Comparing Figs. 3.21 and 3.17a one can now also see the reduction in temperature ranges allowed with the diurnal forcing versus simply using an annual temperature-dependence. All means greater than 21.1°C gave persistence at least for ranges 1.11-4.44 (Fig. 3.17a) with diurnal forcing many of these no longer persist. 35.0°C and 37.9°C give no persistence for any temperature range which is not entirely unexpected given the high mortality rate in high temperatures. The range allowed for a mean of 32.2°C is greatly reduced and the range for 29.4°C is moderately reduced losing two viable ranges. Temperatures 23.9°C and 26.7°C show very similar persistence patterns as before but lose one range. Diurnal forcing has limited the mean temperatures and ranges but in the viable temperatures has actually increased incidence.

The deep troughs that many of the time series went through prompted an examination of the results if a cut-off requirement was added. Simply, if the infected population of the mosquito or host decreased below .0001 then the disease was said to have no chance of recovery and the infected populations of both species were reduced to zero for the remainder of the experiment. One can see the differences here when only annual forcing is utilized and vector mortality as well as EIP are allowed to vary. Again only "boundary" ranges were reduced, but given the first results where no cut off was used (Fig. 3.22b) there are no changes to mean temperatures of 37.8°C and 23.0°C, and 26.7°C only lost one range which showed low incidence to begin with. What is interesting is that the results for mean tempertures 29.4°C, 32.2°C, and 35.0°C each dropped one, one, and two ranges respectively, each of which showed high incidence before the cut off. This implies that the disease reached a very low in-

cidence but was numerically able to regain strength to the point that large epidemics resulted later. A different cut off criteria could have pronounced effects limiting even more ranges which is why the arbitrary cut off of .0001 is so unsatisfying. A stochastic model would better show the possibility of extinction or persistence in these border temperature regions.

The instantiation of a cut-off also affected the persistence in the diurnal fluctuations as seen in Fig. 3.23. An annual range of 15 degrees or larger is no longer capable of sustaining the disease for any mean temperature; A mean of 35°C is no longer able to support the disease for any temperature range and the range at which 32.2°C is able to sustain the disease is greatly reduced. For 26.7°C and 29.4°C, however, only the most extreme temperature range is no longer persisting. The choice for the cut off is arbitrary since a biological population of less than one does not make sense. However, it acts to validate the use of a stochastic model for further examinations.

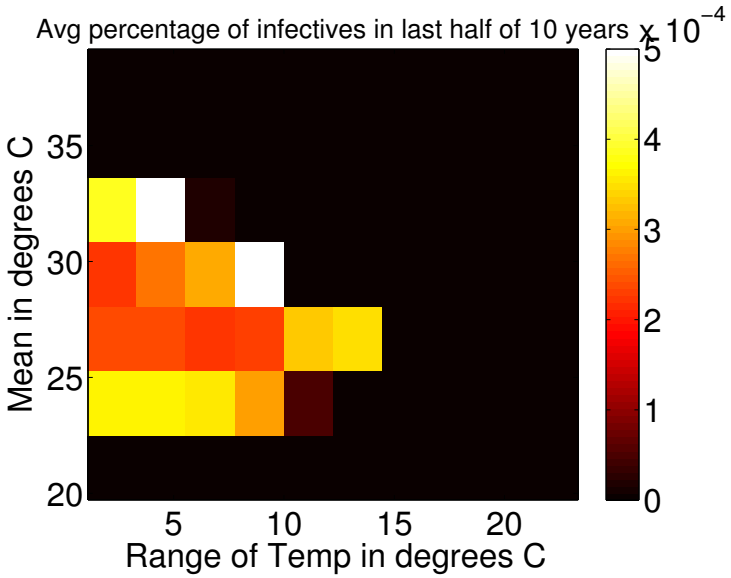

Figure 3.21: Color plot with the average of the last half of the time series for EIP and vector mortality with annual temperature forcing with a diurnal forcing with a temperature range of 9.44°C starting mid-spring

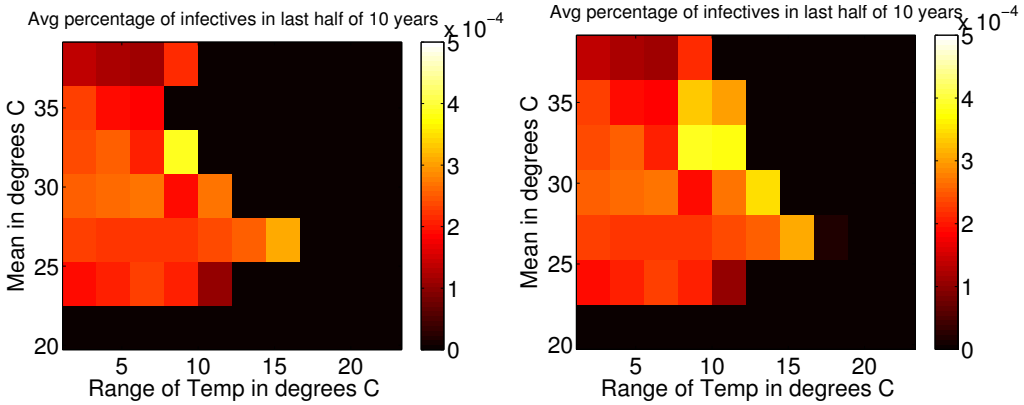

(a) (b)

Figure 3.22: Color plot with the average of the last half of the time series for EIP and vector mortality with annual temperature forcing starting mid-spring. (a) Colorplot of incidence with the rest of the timeseries set to 0 if the number of infected mosquitoes or humans goes below .0001. (b) Colorplot of incidence without the use of a cut-off.

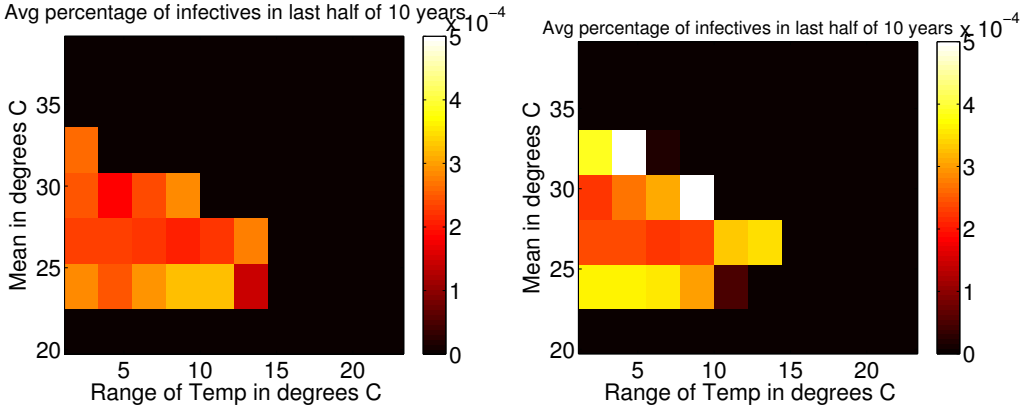

Figure 3.23: Color plot with the average of the last half of the time series for EIP and vector mortality with annual and diurnal temperature forcing starting mid-spring. (a) Colorplot of incidence with the rest of the timeseries set to 0 if the number of infected mosquitoes or humans goes below .0001. (b) Colorplot of incidence without the use of a cut-off.

3.6 Spectral Analysis Data

The spectral analysis results shown here correspond to the settings used in the colorplot seen in Fig. 3.17a. As one can see, there is reasonable agreement between the colorplots showing persistence and the spectral analysis returning a dominant period in the time allowed. There are some discrepancies as seen with a mean of 26.7°C colorplot data allowing persistence at two larger ranges than the table shows, 29.4°C allowing one more range in the table than in the colorplot, and 35.0°C allowing one less range in the table than in the colorplot. These could each be considered "boundary" temperatures and were in half of the cases the temperatures that were shown not to persist if a cut-off was used. Table 3.1 acts as another reference that may indicate persistence and can be useful for observing the underlying periods of oscillation. We often see the expected approximately one year cycle as well as a longer period of six to eight years as was evident in certain time series data (Figs. 3.7 and 3.9). However, it is not only the "boundary" points that may be different from the colorplot to the table.

Table 3.2 and Fig. 3.21 correspond to the same parameters, but there are more differences between the two. A mean temperature of 23.9°C and 29.4°C has one more range in the table versus the colorplot, but the more glaring differences exist in the mean temperatures of 32.2°C, 35.0°C, and 37.8°C. 35.0°C and 37.8°C show no persistence in the plot and are unlikely to persist at these temperatures with diurnal forcing, but now have a dominant period in the allowed time period for no less than six combined temperature ranges. 32.2°C shows dominant periods in the two most extreme temperature ranges in which no mean temperature showed persistence according to the plot. The spectral analysis results can help confirm areas, but also raises new issues of persistence given the deterministic model.

Table 3.1: Spectral analysis data for multiple data EIP, vector mortality taken into account. It begins mid-spring and has annual temperature forcing. Take M as the period corresponding to the frequency with maximum amplitude and S as the period corresponding to the frequency with the second largest amplitude peak, it is presented as M/S in the table. If the period returned is greater than half of the time series' total length of 20 years it is simply represented as T.

Temp	21.1	23.9	26.7	29.4	32.2	35.0	37.8
2	T/T	T/.99	.99/7.81	5.99/.99	.99/5.79	.99/7.18	.99/T
4	T/T	T/.99	.99/8.16	6.19/.99	6.19/.99	7.81/.99	.99/T
6	T/T	T/.99	.99/8.55	6.65/T	7.48/.99	9.98/.99	T/.99
8	T/T	T/8.98	8.98/.99	8.16/4.08	9.98/4.18	8.16/T	T/8.55
10	T/T	T/9.45	9.98/6.19	T/7.48	T/5.79	T/T	T/9.45
12	T/T	T/T	T/8.16	T/9.98	T/T	T/T	T/T
14	T/T	T/T	T/T	T/9.98	T/T	T/T	T/T
16	T/T	T/T	T/T	T/T	T/T	T/T	T/T
18	T/T	T/T	T/T	T/T	T/T	T/T	T/T
20	T/T	T/T	T/T	T/T	T/T	T/T	T/.T

Table 3.2: Spectral analysis for multiple data EIP, vector mortality taken into account. It begins mid-spring and has annual temperature forcing as well as diurnal forcing with a temperature range of 9.44°C. Take M as the period corresponding to the frequency with maximum amplitude and S as the period corresponding to the frequency with the second largest amplitude peak, it is presented as M/S. If the period returned is greater than half of the time series' total length of 20 years it is simply represented as T.

Temp	21.1	23.9	26.7	29.4	32.2	35.0	37.8
2	T/T	T/8.98	7.18/.99	6.91/3.33	T/6.19	T/T	T/T
4	T/T	T/8.98	.99/7.18	7.81/3.90	7.81/T	T/T	T/T
6	T/T	T/8.98	7.81/.99	9.98/4.49	5.61/8.55	T/9.98	T/T
8	T/T	T/8.55	8.16/.99	T/7.81	T/T	T/T	T/T
10	T/T	T/8.55	9.98/4.73	T/9.45	T/T	T/T	T/T
12	T/T	T/9.45	T/7.81	T/T	T/T	T/T	T/T
14	T/T	T/T	T/T	T/T	T/T	T/T	T/T
16	T/T	T/T	T/T	T/T	T/T	T/9.45	T/T
18	T/T	T/T	T/T	T/T	T/9.98	.99/T	.99/T
20	T/T	T/T	T/T	T/T	T/6.41	.99/.49	.99/.49

Chapter 4

Discussion

Average temperatures and temperature ranges that are hospitable to dengue persistence are sensitive to the function used for the EIP as well as vector mortality. The initial conditions also have the potential to impact the dynamics of the system. Considering temperature dependent vector mortality and EIP with annual forcing gives persistence for all temperature averages above 23°C but with limited ranges. When considering diurnal forcing in conjuction with seasonality, regions that allow persistence are further limited (23°C - 34°C with variable ranges). This can be translated to examine dynamics in countries that are currently endemic given specific climate data.

Thailand, Puerto Rico, Mexico and Iquitos, Peru all experience dengue. Thailand has an average temperature of 29°C, but to use the model as we have developed other metrics need to be taken into account. Thailand has summer temperatures that range from 28°C at night to 37°C in the day and winter temperatures that are as low at 15°C at night and rise to 25°C in the day. A DTR of 10.5°C with a yearly mean of 25.5 and range of 11 were used. The time series (Fig. 4.1) with these values show persistence, in the last year of the model the number of infectious humans

ranges from 46.2 to 319. Also by looking at Fig. 3.23, this is well within the range of persistence.

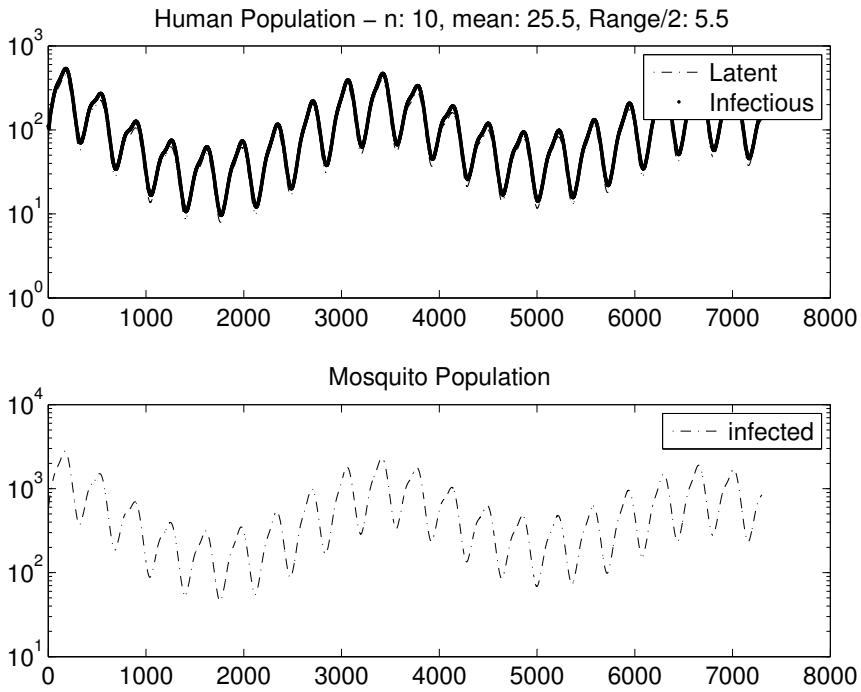

Figure 4.1: Timeseries representative of dengue in Thailand

Puerto Rico has average maximum temperatures ranging from 28.3°C to 31.5°C and average minimum temperatures ranging from 21.3°C to 24.7°C. A DTR of 7 is used with a mean of 25.5°C and a yearly range of 9°C. Persistence is shown in Fig. 4.2; in the final year of the model the population of infectious humans never goes below 67.8 and is as large as 412.1.

Iquitos, Peru has average maximum temperatures ranging from 31.1°C to 32.2°C and average minimum temperatures ranging from 20.0 mydegree to 21.1°C. This results in a much smaller temperature range needed (only 1.1°C) and the mean temp to be 26°C with a DTR of 10°C. This shows persistence in our model given Fig. 4.3,

with a minimum reaching as low as 28.86 at the end of the fourth year. The last year has a maximum of 113.7 infectives and a minimum of 70.53.

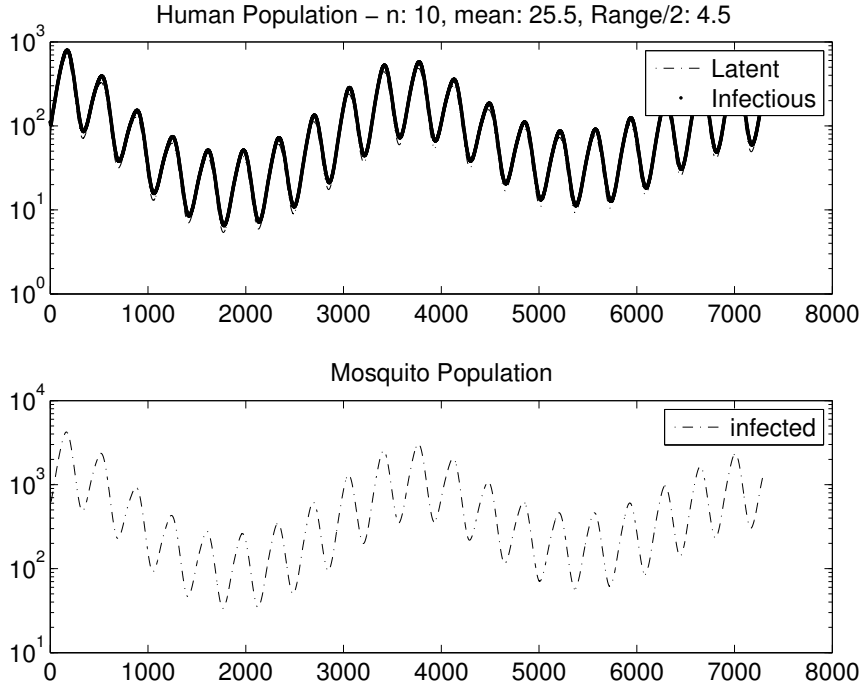

Figure 4.2: Timeseries representative of dengue in Puerto Rico

Mexico is a larger country with a varied terrain and climate so we shall look at two regions that represent temperature extremes. The pacific coastal region of Mexico has average high temperatures of 30.5°C to 32.2°C and average lows ranging from 21.1°C to 23.8°C. This leads to a mean of 26.6°C with a range of 3.33°C and a DTR of 9°C and persistence is once again possible as shown in Fig. 4.4. The infectious human population has a minimum of 63.78 occupants and maximum of 196.7. Northern Mexico, however, has highs that range from 19.4-35°C and lows ranging from 8.8-23.3°C giving a slightly larger DTR of 12°C and a mean of 21.7°C with range of 14°C which does not show persistence given Fig. 4.5. The cut-off population is reached after approximately a year and a half.

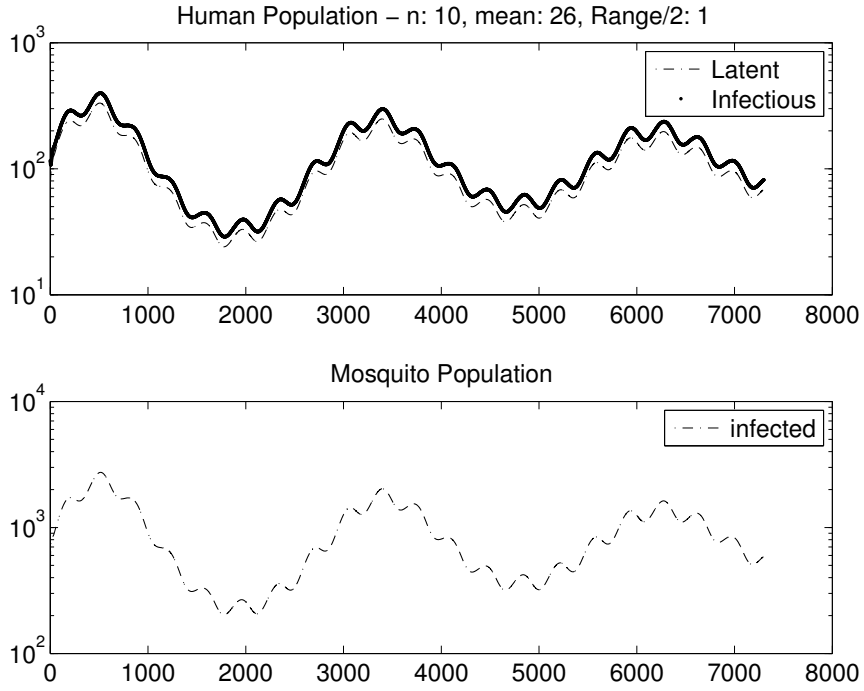

Figure 4.3: Timeseries representative of dengue in Iquitos, Peru

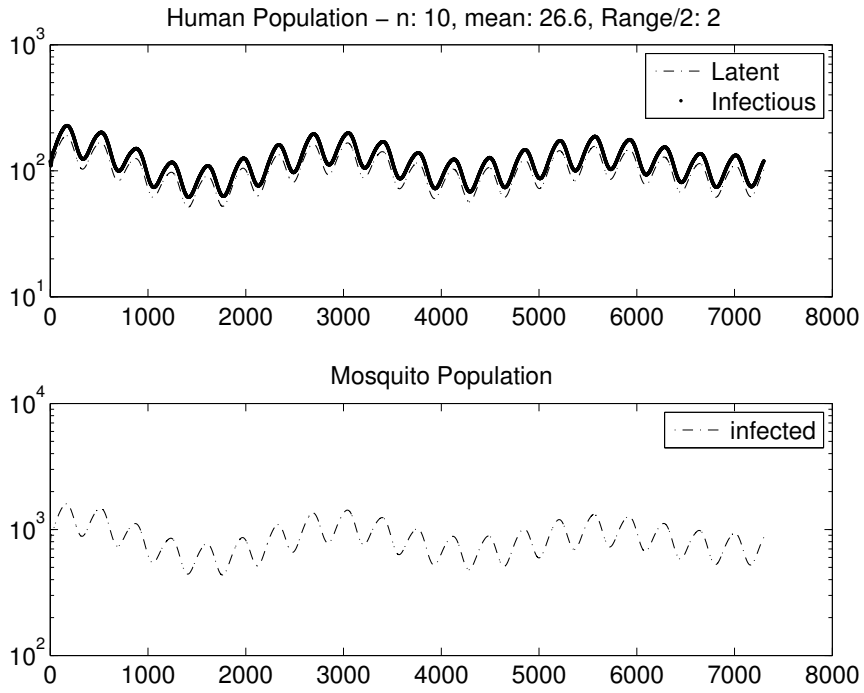

Figure 4.4: Timeseries representative of dengue on the Pacific coast of Mexico

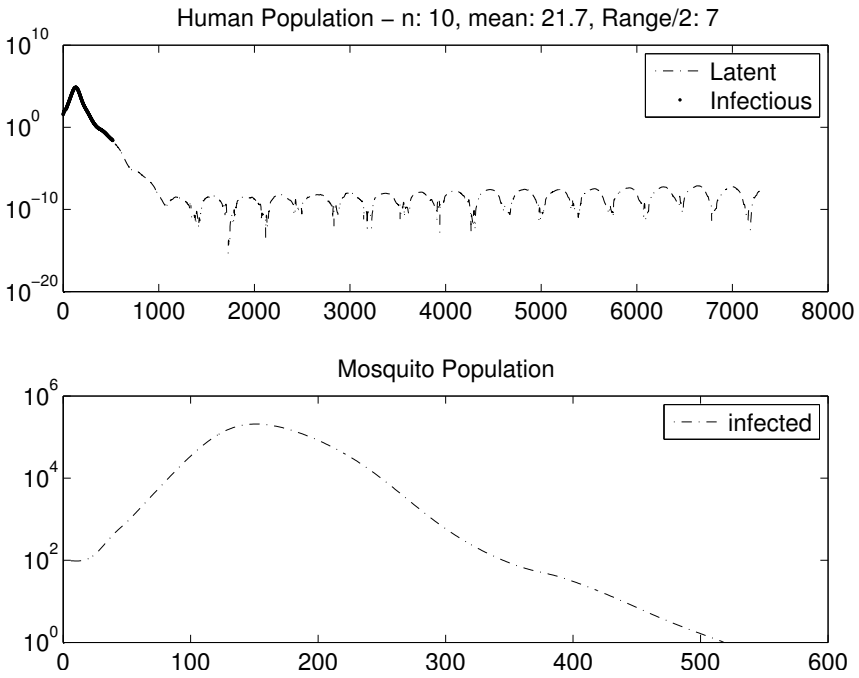

Figure 4.5: Timeseries representative of dengue in Northern Mexico

The model is performing sensibly and with limited data comparison gives reasonable results. It helps to flesh out some of the differences that different regions may experience given differing climate and temperature norms. The model could be improved greatly with the development of a stochastic model. This modification would require different code for the framework of the model but the parameters and structure would be consistent with what has already been done. This addition could more clearly define where persistence is much more probable and the conditions where the disease would instead go extinct.

It is also clear that the daily temperature contributes greatly. Having a temperature dependent model without diurnal fluctuations omits key interactions and leads to wrong conclusions about potential regions of persistence. This is also supported by the recent work done by Lambrechts *et al.* [26] in which they found that the diurnal fluctuations have the potential to shorten EIP, but so far this is unsupported by field data. A further improvement could be made by using a more realistic daily temperature curve instead of the sine function. One such function is presented in Paaijmans [34], but this would necessitate interpolation and could drastically increase the computation time needed.

What is most clear is that more data are needed in terms quality and quantity; for both the extrinsic incubation period and the vector mortality. Both of these parameters contribute greatly to the overall transmissibility of dengue. They interact in a non-linear fashion, and thus both parameters need more data points to give greater resolution for the fitted function as well as error estimates for each temperature.

References

[1] RM Anderson and RM May. *Infectious Diseases of Humans: Dynamics and Control*. Oxford University Press, Oxford, 1991.

[2] S Atmosoed, JS Saroso, and PF Vanpeene et al. Man-biting activity of *Aedes-aegypti* in Jakarta, Indonesia. *Mosquito News*, 32:467–469, 1972.

[3] P Barbazan, M Guiserix, and W Boonyuan et al. Modeling the effect of temperature on transmission of dengue. *Medical and Veterinary Entomology*, 24:66–73, 2010.

[4] LM Bartley, CA Donnelly, and GP Garnett. The seasonal pattern of dengue in endemic areas: mathematical models of mechanisms. *Transactions of the Royal Society of Tropical Medicine and Hygiene*, 96:387–397, 2002.

[5] SC Chen, CM Liao, and CP Chio et al. Lagged temperature effect with mosquito transmission potential explains dengue variability in southern Taiwan: Insights from a statistical analysis. *Science of the Total Environment*, 408:4069–4075, 2010.

[6] G Chowell, P Diaz-Duenas, and JC Miller et al. Estimation of the reproduction number of dengue fever from spatial epidemic data. *Mathematical Biosciences*, 208:571–589, 2007.

[7] G Chowell and F Sanchez. Climate-based descriptive models of dengue fever: The 2002 epidemic in Colima, Mexico. *Journal of Environmental Health*, 68:40–44, 2006.

[8] GR Conway, M Trpis, and GA Mcclella. Population parameters of mosquito *Aedes-aegypti*(l) estimated by mark-release-recapture in a suburban habitat in Tanzania. *Journal of Animal Ecology*, 43:289–304, 1974.

[9] EAPD Costa, EMD Santos, and JC Correia et al. Impact of small variations in temperature and humidity on the reproductive activity and survival of *Aedes aegypti* (Diptera, Culicidae). *Revista Brasileira De Entomologia*, 54:488–493, 2010.

[10] C Dye. Models for the population-dynamics of the yellow-fever mosquito, *Aedes-aegypi*. *Journals of Animal Ecology*, 53:247–268, 1984.

[11] RA Erickson, SM Presley, and LJS Allen et al. A dengue model with a dynamic *Aedes albopictus* vector population. *Ecological Modelling*, 221:2899–2908, 2010.

[12] RA Erickson, SM Presley, and LJS Allen et al. A stage-structured, *Aedes albopictus* population model. *Ecological Modelling*, 221:1273–1282, 2010.

[13] DA Focks, E Daniels, and DG Haile Et Al. A simulation-model of the epidemiology of urban dengue fever - literature analysis, model development, preliminary validation, and samples of simulation results. *American Journal of Tropical Medicine and Hygiene*, 53:489–506, 1995.

[14] DA Focks, DG Haile, and E Daniels et al. Dynamic life table model for *Aedes-aegypi* (Diptera, Culcidae) - analysis of the literature and model development. *Journal of Medical Entomology*, 30:1003–1017, 1993.

[15] DA Focks, DG Haile, and E Daniels et al. Dynamic life table model for *Aedes-aegypi* (Diptera, Culicidae) - simulation and validation. *Journal of Medical Entomology*, 30:1018–1028, 1993.

[16] DJ Gubler. *Aedes-aegypi* and *Aedes-aegypi*-borne disease-control in the 1990s - top down or bottom up. *American Journal of Tropical Medicine and Hygiene*, 40:571–578, 1989.

[17] S Hales, N de Wet, and J Maindonald et al. Potential effect of population and climate changes on global distribution of dengue fever: an empirical model. *Lancet*, 360:830–834, 2002.

[18] SB Halstead. Dengue virus - mosquito interactions. *Annual Review of Entomology*, 53:273–291, 2008.

[19] SP Hatchett. Winter survival of *Aedes-aegypi* (l) in Houston, Tex. *Public Health Reports*, 61:1234–1244, 1946.

[20] MA Johansson, DAT Cummings, and GE Glass. Multiyear climate variability and dengue-El Niño Southern Oscillation, weather, and dengue incidence in Puerto Rico, Mexico, and Thailand: A longitudinal data analysis. *Plos Medicine*, 6, 2009.

[21] JC Jones and DR Pilitt. Blood-feeding behavior of adult *Aedes-aegypi* mosquitos. *Biological Bulletin*, 145:127–139, 1973.

[22] MJ Keeling and P Rohani. *Modeling Infectious Diseases in Humans and Animals*. Princeton University Press, Princeton, 2008.

[23] MM Khin and KA Than. Trans-ovarial transmission of dengue-2 virus by *Aedes-aegypi* in nature. *American Journal of Tropical Medicine and Hygiene*, 32:590–594, 1983.

[24] AM Kilpatrick, MA Meola, and RM Moudy et al. Temperature, viral genetics, and the transmission of West Nile virus by *Culex pipiens* mosquitoes. *Plos Pathogens*, 4, 2008.

[25] LW Lai. Influence of environmental conditions on asynchronous outbreaks of dengue disease and increasing vector population in Kaohsiung, Taiwan. *International Journal of Environmental Health Research*, 21:133–146, 2011.

[26] L Lambrechts, PP Krijn, and F Thanyalak et al. Impact of daily temperature fluctuations on dengue virus transmission by *Aedes aegypti*. *Proceedings of the National Academy of Sciences of the United States of America*, 108:7460–7465, 2011.

[27] C Lansdowne and CS Hacker. Effect of fluctuating temperature and humidity on adult life table characteristics of 5 strains of *Aedes-aegypi*. *Journal of Medical Entomology*, 11:723–733, 1975.

[28] R Lowe, TC Bailey, and DB Stephenson et al. Spatio-temporal modelling of climate-sensitive disease risk: Towards an early warning system for dengue in Brazil. *Computers and Geosciences*, 37:371–381, 2011.

[29] WHR Lumsden. Observations on the effect of microclimate on biting by *Aedes-aegypi* (l) (Dipt Culicid). *Journal of Experimental Biology*, 24:361–373, 1947.

[30] DM McLean, AM Clarke, and JC Coleman et al. Vector capability of *Aedes-aegypi* mosquitoes for California encephalitis and dengue viruses at various temperatures. *Canadian Journal of Microbiology*, 20:255–261, 1974.

[31] MJ Nelson, LS Self, and CP Pant Et Al. Diurnal periodicity of attraction to human bait of *Aedes-aegypi* (Diptera Culicidae) in Jakarta, Indonesia. *Journal of Medical Entomology*, 14:504–510, 1978.

[32] World Health Organization. `http://www.who.int/mediacentre/factsheets/fs117/en/index.html`. Online; accessed 23-May-2011.

[33] M Otero and HG Solari. Stochastic eco-epidemiological model of dengue disease transmission by *Aedes-aegypi* mosquito. *Mathematical Biosciences*, 223:32–46, 2010.

[34] KP Paaijmans, AF Read, and MB Thomas. Understanding the link between malaria risk and climate. *Proceedings of the National Academy of Sciences of the United States of America*, 106:13844–13849, 2009.

[35] AH Parker. The effect of a difference in temperature and humidity on certain reactions of female *Aedes-aegypi* (l). *Bulletin of Entomological Research*, 43:221–229, 1952.

[36] WK Reisen, Y Fang, and VM Martinez. Effects of temperature on the transmission of West Nile virus by Culex tarsalis (Diptera : Culicidae). *Journal of Medical Entomology*, 43:309–317, 2006.

[37] A Rohani, YC Wong, and I Zamre et al. The effect of extrinsic incubation temperature on development of dengue serotype 2 and 4 viruses in *Aedes-aegypi* (l.). *Southeast Asian Journal of Tropical Medicine and Public Health*, 40:942–950, 2009.

[38] HF Schoof. Mating resting habits and dispersal of *Aedes-aegypi*. *Bulletin of the World Health Organization*, 36:600–601, 1967.

[39] TW Scott, AC Morrison, and LH Lorenz et al. Longitudinal studies of *Aedes-aegypi* (Diptera : Culicidae) in Thailand and Puerto Rico: Population dynamics. *Journal of Medical Entomology*, 37:77–88, 2000.

[40] JF Siler, MW Hall, and AP Hitchens. Transmission of dengue fever by mosquitoes. *Proceedings of the Society for Experimental Biology and Medicine*, 23:197–201, 1925.

[41] GC Smith, DA Eliason, and CG Moore Et Al. Use of elevated-temperatures to kill *Aedes-albopictus* and *Aedes-aegypi*. *Journal of the American Mosquito Control Association*, 4:557–558, 1988.

[42] WW Smith and GJ Love. Winter and spring survival of *Aedes-aegypi* in Southwestern Georgia. *American Journal of Tropical Medicine and Hygiene*, 7:309–311, 1958.

[43] RS Soman. Studies on diel periodicity in landing of *Aedes-aegypi* on man in Bangalore City. *Indian Journal of Medical Research*, 67:937–941, 1978.

[44] FL Soper. Dynamics of *Aedes-aegypi* distribution and density - seasonal fluctuations in Americas. *Bulletin of the World Health Organization*, 36:536–538, 1967.

[45] DM Watts, DS Burke, and BS Harrison et al. Effect of temperature on the vector efficiency of *Aedes-aegypi* for dengue-2 virus. *American Journal of Tropical Medicine and Hygiene*, 36:143–152, 1987.

[46] HJ Wearing, P Rohani, TC Cameron, and SM Sait. The dynamical consequences of developmental variability and demographic stochasticity for host-parasitoid interactions. *The American Naturalist*, 164:543–558, 2004.

[47] HM Yang, MDD Macoris, and KC Galvani et al. Follow up estimation of *Aedes-aegypi* entomological parameters and mathematical modellings. *Biosystems*, 103:360–371, 2011.

[48] HM Yang, MLG Macoris, and KC Galvani et al. Assessing the effects of temperature on dengue transmission. *Epidemiology and Infection*, 137:1179–1187, 2009.

[49] HM Yang, MLG Macoris, and KC Galvani et al. Assessing the effects of temperature on the population of *Aedes-aegypi*, the vector of dengue. *Epidemiology and Infection*, 137:1188–1202, 2009.

[50] M Yasuno and RJ Tonn. Study of biting habits of *Aedes-aegypi* in Bangkok-Thailand. *Bulletin of the World Health Organization*, 43:319–325, 1970.